BBA - Molecular Cell Research 1871 (2024) 119585

Contents lists available at ScienceDirect

BBA - Molecular Cell Research

journal homepage: www.elsevier.com/locate/bbamcr

Research paper

Opposite regulation of glycogen metabolism by cAMP produced in the cytosol and at the plasma membrane

Paulo F.V. Bizerra [a,b], Eduardo H. Gilglioni [a,c], Hang Lam Li [a,d], Simei Go [a,d,e], Ronald P.J. Oude Elferink [a,d], Arthur J. Verhoeven [a], Jung-Chin Chang [a,d,f,*]

[a] Tytgat Institute for Liver and Intestinal Research, Amsterdam UMC, University of Amsterdam, Amsterdam, the Netherlands
[b] State University of Maringá, Paraná, Brazil
[c] Signal Transduction and Metabolism Laboratory, Université Libre de Bruxelles, Brussels, Belgium
[d] Amsterdam Gastroenterology Endocrinology Metabolism (AGEM) Research Institute, Amsterdam UMC, University of Amsterdam, Amsterdam, the Netherlands
[e] Department of Oncology, University of Oxford, Oxford, United Kingdom
[f] Division of Cell Biology, Metabolism & Cancer, Department of Biomolecular Health Sciences, Faculty of Veterinary Medicine, Utrecht University, Utrecht, the Netherlands

ARTICLE INFO

Keywords:
Cyclic AMP
Glycogenolysis
Glycogen breakdown
Soluble adenylyl cyclase
Exchange protein directly activated by cAMP (Epac)
cAMP signaling microdomains

ABSTRACT

Cyclic AMP is produced in cells by two different types of adenylyl cyclases: at the plasma membrane by the transmembrane adenylyl cyclases (tmACs, *ADCY1~ADCY9*) and in the cytosol by the evolutionarily more conserved soluble adenylyl cyclase (sAC, *ADCY10*). By employing high-resolution extracellular flux analysis in HepG2 cells to study glycogen breakdown in real time, we showed that cAMP regulates glycogen metabolism in opposite directions depending on its location of synthesis within cells and the downstream cAMP effectors. While the canonical tmAC-cAMP-PKA signaling promotes glycogenolysis, we demonstrate here that the non-canonical sAC-cAMP-Epac1 signaling suppresses glycogenolysis. Mechanistically, suppression of sAC-cAMP-Epac1 leads to Ser-15 phosphorylation and thereby activation of the liver-form glycogen phosphorylase to promote glycogenolysis. Our findings highlight the importance of cAMP microdomain organization for distinct metabolic regulation and establish sAC as a novel regulator of glycogen metabolism.

1. Introduction

Since the discovery of 3′,5′-cyclic adenosine monophosphate (cAMP) as the second messenger in hormone-mediated glycogenolysis [1–3], nine transmembrane adenylyl cyclases (tmACs, *ADCY1~ADCY9*) have been identified as sources of this versatile second messenger at the plasma membrane (reviewed in [4]). Much later, a distinct type of mammalian adenylyl cyclase, soluble adenylyl cyclase (sAC, *ADCY10*), was discovered in the cytosol [5]. sAC is evolutionarily more conserved than tmACs and is not localized at the plasma membrane but exclusively in the cytoplasm [6,7]. cAMP produced in the cytosol by sAC and at the plasma membrane by tmACs share the same cAMP effectors, including protein kinase A (PKA) and "exchange factor directly activated by cAMP" (Epac1 and Epac2). However, in contrast to tmACs, sAC is neither regulated by G-proteins nor activated by forskolin, a broad-spectrum tmAC activator [5,6]. Rather, sAC is activated by bicarbonate and ATP in the physiological ranges and fine-tuned by the free Ca^{2+} concentration [6,8–11]. Different localizations for intracellular sAC have been suggested, including mitotic spindles, nuclei [12], and mitochondria [12,13].

While the tmACs are evolved in multicellular organisms and are activated or inhibited by signaling of hormones and neurotransmitters to mediate intercellular communication, the bicarbonate-sensitive sAC homologs are conserved in both multicellular and unicellular organisms and serve more cell-autonomous functions [7,14,15]. Firstly, sAC regulates oxidative phosphorylation by sensing bicarbonate derived from CO_2 produced by the tricarboxylic acid cycle [13] and free Ca^{2+} in the mitochondrial matrix [16]. Secondly, sAC is an ATP sensor due to its high K_m for ATP (ranging from 1 to 10 mM) [8,11,17]. Thirdly, Ca^{2+}, another versatile and universal second messenger, stimulates sAC in synergy with bicarbonate [9,17], allowing sAC to fine-tune cellular metabolism. Importantly, sAC is expressed in almost all tissues

* Corresponding author at: Division of Cell Biology, Metabolism & Cancer, Department of Biomolecular Health Sciences, Faculty of Veterinary Medicine, Utrecht University, Utrecht, the Netherlands.
E-mail addresses: j.chang1@uu.nl, j.chang@amsterdamumc.nl (J.-C. Chang).

https://doi.org/10.1016/j.bbamcr.2023.119585
Received 24 March 2023; Received in revised form 5 September 2023; Accepted 6 September 2023
Available online 14 September 2023

examined [9,18]. We have recently shown that sAC acts as an acute switch between aerobic glycolysis and oxidative phosphorylation maintaining the autonomous energy metabolism of cells [19].

Over the past two decades, accumulating evidence supports that the versatility of cAMP signaling is based on the compartmentalization of cAMP signaling [7,20,21]. Optical mapping of G-protein-coupled receptor (GPCR)-dependent cAMP signaling reveals that individual GPCRs generate independent receptor-associated cAMP nanodomains [22]. From its site of generation, cAMP concentration quickly decays due to buffering by regulatory units of PKA [23] and degradation by phosphodiesterases (PDEs), thereby creating a signaling microdomain [24–26]. The spatial specificity is further enhanced by the liquid-liquid separation of the regulatory subunit of PKA [27] and by scaffolding proteins, such as A-kinase anchoring proteins [28,29] that assemble adenylyl cyclases, PDEs, and cAMP effectors at the same location. Indeed, cAMP generated at the plasma membrane by tmACs and cAMP generated in the cytosol by sAC or bacterial adenylyl cyclases can exert opposite regulation of apoptosis [30,31] and endothelial barrier function [32,33]. Although it is well-established that tmAC-derived cAMP activates PKA, which induces a phosphorylation cascade of phosphorylase kinase and glycogen phosphorylase to induce glycogenolysis [2,3,34,35], sAC-derived cAMP has also been implicated in affecting glycogen levels in astrocytes [36,37]. However, it is unknown whether sAC-derived cAMP and tmAC-derived cAMP regulate glycogen metabolism by different mechanisms and, if so, how the specificity of cAMP signaling is maintained in the same cell. In the present study, we applied high-resolution extracellular flux analysis to study glycogen breakdown in real-time and revealed opposite regulation of glycogen metabolism by sAC-derived cAMP and tmAC-derived cAMP. While the well-established tmAC-cAMP-PKA signaling axis promotes glycogenolysis, we show here a hitherto unknown regulation of glycogenolysis by a sAC-cAMP-Epac1 signaling axis.

2. Materials and methods

2.1. Materials

Unless otherwise indicated, materials were purchased from Sigma-Aldrich.

2.2. Cell culture

The immortalized human intrahepatic cholangiocytes H69 (hereafter H69 cholangiocytes) was a kind gift from Dr. Douglas Jefferson [38] and was cultured in DMEM/F-12 (3:1) with hormonal supplements as described previously [30]. HepG2, Caco-2, HeLa, HEK293T, and Madin-Darby canine kidney (MDCK) cells were cultured in DMEM (Invitrogen), supplemented with 2 g/L glucose, 1.8 g/L $NaHCO_3$, 20 mM HEPES-NaOH pH 7.4 and 10 % fetal bovine serum. For all experiments, cells were refreshed the day before the experiment.

2.3. Extracellular flux analysis

Extracellular acidification rate (ECAR) and oxygen consumption rate (OCR) were measured with a Seahorse XF96 Analyzer (Agilent, United States). HepG2 cells were cultured in a 96-well Seahorse culture plate until confluence. Media were refreshed the day before the experiment. On the day of the experiment, cells were pre-incubated for 1 h at 37 °C in the experimental medium, which was based on a modified Hank's balanced salt solution (HBSS) for ambient air (please refer to Table S1 for formulation) supplemented with 0.1 % fatty acid-free bovine serum albumin (BSA). During this pre-incubation the indicated substrates or inhibitors (2-deoxyglucose and glycogen phosphorylase *a* inhibitor CP-91149) were added. Twenty-five microliters of concentrated compound solutions prepared in the experimental medium (without BSA) were injected sequentially as indicated in the figures. The final concentrations of compounds used in this study were as follows: forskolin, 1 μM; LRE1, 50 μM; (*R*)-CE3F4, 50 μM; ESI-05, 10 μM; H89, 10 μM; oligomycin A, 2.5 μM; FCCP, 2 μM; antimycin A, 2.5 μM; rotenone, 1 μM. The coupled mitochondrial respiration rate was defined as the difference between the average of the last three OCR measurements after the addition of inhibitors or vehicle control and the last OCR measurement after the addition of oligomycin A. The FCCP-driven mitochondrial respiration rate was defined as the difference between the first OCR measurement after FCCP addition and the last OCR measurement after the addition of oligomycin A.

2.4. Estimation of ATP production rates by glycolysis and by mitochondria using extracellular flux measurements

The time-lapsed ATP production rates were calculated from extracellular fluxes (ECARs and OCRs) as elegantly described [39,40]. Since cells were pre-incubated in HBSS until reaching a steady state and before imposing the acute perturbation of sAC activity, it was assumed that the oxidation of the provided substrates in the mitochondria was complete and that the contribution from other endogenous substrates (except for glycogen) was negligible. Because cells were fueled solely with octanoate, the glycolytic flux was assumed to come from glycogenolysis. The total ATP production rate (J_{ATP_total}) is defined as the sum of the ATP production rate of glycolysis ($J_{ATP\_glycolysis}$, substrate level phosphorylation by phosphoglycerate kinase and pyruvate kinase) and the ATP production rate of mitochondria ($J_{ATP\_mitochondria}$, substrate level phosphorylation by succinyl-CoA synthetase in the TCA cycle and oxidative phosphorylation by the electron transport chain and ATP synthase). Further details of the calculation of ATP production rates are given in [19]. The values of maximal H^+/O_2, ATP/lactate, maximal P/O ratios with octanoate and glycogen as bioenergetic substrates are given in Table S2.

2.5. Sample preparation for the enzymatic determination of glycogen

At the end of the incubation, cells were washed twice with ice-cold PBS and lysed in TTE buffer (1 % Triton X-100, 10 mM Tris-HCl pH 8.0 and 1 mM EDTA-NaOH, pH 8.0) or RIPA buffer (150 mM NaCl, 20 mM Tris-HCl pH 8.0, 1 % Triton X-100, 0.1 % SDS, 0.5 % Na-deoxycholate). Lysates were centrifuged at 20,000 ×*g* at 4 °C for 10 min. Supernatants were harvested for determination of glycogen and protein concentrations. For the determination of glycogen, 50 μL of supernatant was mixed with 20 μL 0.35 M NaOH and heated at 80 °C for 30 min to degrade monosaccharides. The hot alkali-treated lysates were then deproteinized by adding 30 μL 10 % (*w/v*) metaphosphoric acid (MPA) and incubated on ice for at least 1 h or overnight at 4 °C. Samples were centrifuged at 20,000 ×*g* for 10 min. Twenty microliters of deproteinized samples or glucose standards (prepared in 3 % MPA) were mixed with 100 μL solution A (2.5 U/mL amyloglucosidase from *Aspergillus niger*, 50 mM K_2HPO_4-KH_2PO_4, pH 8.0). The resulting mixture had a pH of about 4.7, which is optimal for amyloglucosidase to hydrolyze glycogen to glucose. After 1-h incubation at 45 °C, 50 μL solution B (1.5 mM homovanillic acid, 2 U/mL horseradish peroxidase, 0.5 M K_2HPO_4-KH_2PO_4, pH 8.0) was added to correct the pH to 6.8 to enable subsequent measurement of the glucose by glucose oxidase. After determining the background fluorescence at $\lambda_{ex}/\lambda_{em}$ = 320/450 nm in the CLARIOstar microplate reader (BMG LABTECH, Ortenberg, Germany), 50 μL start solution (8 U/mL glucose oxidase) was added and the fluorescence was followed every 2 min until the reaction was complete (within 1 h).

2.6. Isolation and culture of primary mouse hepatocytes

Animal experiments were approved by the institutional animal experiment committee. Primary mouse hepatocytes were isolated from wild-type male C57BL/6J mice after overnight ad libitum feeding by a

two-step collagenase perfusion method through the portal vein. Cells were cultured in collagen sandwich configuration overnight on a 60-rpm shaking platform in a 5 % CO_2, 37 °C incubator. The isolation procedure and culture of primary mouse hepatocytes were performed as described [41].

2.7. Sample preparation and enzymatic determination of lactate and pyruvate in the medium

Cells were refreshed with the full culture medium one day prior to the experiment. On the day of the experiment, the medium was changed to the experimental medium (composition given in Table S1) supplemented with 5.5 mM glucose and 0.1 % fatty acid-free bovine serum albumin (BSA). At the start of the experiment, cells were exposed to media containing the indicated inhibitors and vehicle controls. At indicated time points, 50 μL of spent medium was mixed with 75 μL ice-cold 5 % (*w/v*) meta-phosphoric acid (MPA) for deproteinization. After incubating for at least 1 h at 4 °C, the MPA-acidified samples were centrifuged at 20,000 ×*g* for 10 min. The supernatants were harvested. Lactate and pyruvate are stable in 3 % MPA at 4 °C for at least 1 month and was assayed directly from the MPA extracts. L-Lactate was determined enzymatically with the L-lactate dehydrogenase method and pyruvate with the pyruvate oxidase method as previously described [41].

2.8. Determination of ATP, ADP, and AMP by high-performance liquid chromatography (HPLC) for the cytosolic adenylate energy charge

HepG2 cells were treated with 0.1 % DMSO or 50 μM sAC-specific inhibitor LRE1 in HBSS containing indicated substrates. After indicated period of incubation, cytosolic metabolites were extracted with permeabilization buffer (120 mM KCl, 10 mM NaCl, 5 mM EDTA, 20 mM HEPES, pH 7.1) containing 100 μg/mL digitonin. Two hundred microliter of digitonin extracts were mixed with 16 μL 70 % perchloric acid for deproteinization and subsequently neutralized with 2.5 M K_2CO_3. The neutralized perchloric acid extracts of HepG2 cells were then analyzed for AMP, ADP and ATP by high-performance liquid chromatography using a Partisphere SAX column (Whatman International Ltd.) exactly as described [42]. Adenylate energy charge was defined as ([ATP] + 0.5 × [ADP]) / ([ATP] + [ADP] + [AMP]) according to Atkinson and Walton [43].

2.9. Sodium dodecyl sulfate–polyacrylamide gel electrophoresis (SDS-PAGE) and Western blotting

Protein concentrations of whole cell lysates in RIPA buffer supplemented with 5 mM EDTA, cOmplete™ protease inhibitor cocktail, PhosSTOP™ phosphatase inhibitor cocktail, and 10 mM NaF. Protein content was quantified by bicinchoninic acid (BCA) assay. Equal amount of protein (40–50 μg) was subjected to SDS-PAGE, transferred to polyvinylidene difluoride (PVDF) membranes by semi-dry blotting and blocked overnight in 5 % non-fat milk/PBST (phosphate-buffered saline with 0.05 % (*w/v*) Tween 20) at 4 °C. For immunodetection, the PVDF membranes were incubated with primary antibody for 1 h, washed 3 times with TBST (Tris-buffered saline with 0.05 % (*w/v*) Tween 20), incubated with horseradish peroxidase-conjugated secondary antibody for 1 h, and washed again 4 times with TBST. All antibodies were diluted in 1 % non-fat milk-TBST and incubation was performed at room temperature. The PVDF membrane was developed with homemade enhanced chemiluminescence reagents (100 mM Tris-HCl pH 8.5, 1.25 mM luminol, 0.2 mM p-coumarin and freshly added 3 mM H_2O_2) and detected using the ImageQuant LAS 4000 (GE Healthcare Life Sciences). The signal intensity was quantified by densitometry using the ImageJ software. Please refer to Table S3 for the list of primary and secondary antibodies and dilution.

2.10. Cloning and lentivirus-mediated knockdown and inducible overexpression of human sAC

The pLKO.1 – TRC cloning vector is a kind gift from Prof. David Root (Addgene plasmid # 10878) [44]. The cloning of lentiviral shRNA constructs against human sAC was performed essentially as previously described [19]. Briefly, the stuffer of pLKO.1 was removed by sequential digestion with *Age*I and *Eco*RI to generate the open vector of pLKO.1. The sense and anti-sense oligonucleotides for control shRNA (SHC) and sAC-targeting shRNAs (sACKD #128, #1280, #1388) were annealed and ligated to the open vector of pLKO.1 to generate the control and the sACKD lentiviral constructs.

For doxycycline-inducible over-expression of the human truncated sAC isoform (as described by Geng et al. [9]), the Cas9 sequence was removed from the pCW-Cas9-Puro lentiviral vector (a gift from Prof. Eric Lander & Prof. David Sabatini, Addgene plasmid # 50661) by *Nhe*I and BamHI digestion. The sense and anti-sense oligonucleotides for a multiple cloning site (MCS) was annealed and ligated to the open vector to generate the pCW-MCS-Puro construct with stop codons for all reading frames after the MCS. The truncated human sAC isoform (htsAC) was PCR cloned from a pcDNA-htsAC plasmid (a kind gift from Prof. Orsen Moe) [9]. Both the htsAC and pCW-MCS-puro were digested with *Age*I and BamHI and then ligated together to generate the pCW-htsAC-His_6-Puro construct.

All constructs were verified by restriction enzyme analysis and sequencing. The production of lentiviruses and the lentiviral transduction were performed essentially as previously described [30]. Briefly, HepG2 cell were transduced with lentivirus carrying the pCW-htsAC-His_6-Puro construct in the presence of 10 μg/mL diethylaminoethyl-dextran (DEAE-dextran) and selected with 2.5 μg/mL puromycin to generate the $HepG2^{pCW\text{-}htsAC\text{-}His6}$ cells that over-express the human truncated sAC upon doxycycline treatment. The control cell line $HepG2^{pCW\text{-}Empty}$ was generated in parallel using lentivirus carrying the pCW-MCS-Puro construct. To induce htsAC expression, cells were incubated overnight with 0.8 μg/mL doxycycline hyclate. Because constitutive sAC knockdown severely interfered with cell proliferation, HepG2 cells were acutely transduced with lentivirus carrying control shRNA and sACKD shRNA #1388 without puromycin selection. Our previous result showed that sAC is a short-lived protein [45] and that sACKD shRNA #1388 induced significant down-regulation of sAC after 48 h [30]; therefore, experiments of sAC knockdown HepG2 cells were performed 48 h after the lentiviral transduction.

The sense and anti-sense oligonucleotides for the control and anti-sAC shRNAs, multiple cloning sites, and PCR cloning primers are given in Table S4.

2.11. cAMP accumulation assay

HepG2 cells or human H69 cholangiocytes were cultured in 24-well plates until near confluency and refreshed the day before experiments. To induce htsAC expression, $HepG2^{pCW\text{-}htsAC\text{-}His6}$ and $HepG2^{pCW\text{-}Empty}$ cells were refreshed with the full medium supplemented with 0.8 μg/mL doxycycline hyclate. On the day of the experiment, cells were pre-equilibrated in 200 μL experimental medium (FBS-free DMEM with 5.5 mM glucose, 4 mM glutamine, and 1 mM pyruvate) for at least 1 h in 5 % CO_2, 37 °C incubator. All compounds were diluted in the experimental medium. Immediately before the start of experiment, 3 wells of untreated cells were harvested for baseline cAMP determination by adding *in order* 100 μL 3.5× lysis solution (1× lysis solution = 0.1 M HCl/1 % Triton X-100), 25 μL of 10× vehicle control (1× = 0.1 % DMSO), and 25 μL of 10 × 3-isobutyl-1-methylxanthine (IBMX, 1× = 0.5 mM IBMX).

For determining cAMP production, 25 μL 10× LRE1 (1× = 50 μM LRE1) and 10× vehicle control (1× = 0.1 % DMSO) were added to cells and mixed immediately by shaking. After 5 min pre-incubation, 25 μL of 10× IBMX was added to start cAMP accumulation by inhibiting the

cAMP-degrading phosphodiesterases. After 10 to 15 min, the cAMP accumulation was terminated by adding 100 μL 3.5× lysis solution. The acid lysates were cleared by centrifuging at 20,000 x g, 4 °C for 10 min. The cAMP content of the acid lysate was determined by a competitive ELISA using the Direct cAMP ELISA kit (Enzo Life Sciences ADI-901-066). The cAMP standards for the competitive ELISA were prepared in a modified assay diluent (2.5 parts experimental medium and 1 part 3.5× lysis solution) to account for the background composition of the samples. The protein content of the acid lysates was determined by the bicinchoninic acid (BCA) assay and corrected against the blank medium. The accumulated cAMP was corrected for the baseline value and then normalized to the protein content.

2.12. Statistics

All results are given as mean ± standard deviation (SD). Statistical significance was determined by two-tailed Student's *t*-test, one-way analysis of variance (ANOVA) with Tukey's or Dunnett's multiple comparison test, or two-way ANOVA with Sidak's multiple comparison test as indicated in the legends. Statistical analysis was performed with GraphPad Prism 7 (GraphPad Software, La Jolla, CA) with an α error of 0.05.

3. Results

3.1. Inhibition of soluble adenylyl cyclase in the absence of glucose causes a transient stimulation of glycolysis in HepG2 cells

To investigate the possible role of sAC in glycogen metabolism, we first made use of the Seahorse flux analyzer which measures in real time not only the oxygen consumption rate (OCR) of cells, but also the extracellular acidification rate (ECAR). Although both glycolysis and TCA cycle activity contribute to ECAR, glycolytic flux accounts for the majority of ECAR [39,40]. ECAR thus represents a good first estimation of glycolytic flux. In the absence of added glucose, glucose units for glycolysis are mostly derived from glycogen breakdown and in this condition ECAR could be a good indicator of glycogenolysis. Indeed, when HepG2 cells were incubated with octanoate (a membrane-permeable fatty acid substrate for mitochondrial β-oxidation) and subsequently stimulated with the tmAC activator forskolin, we observed a clear increase in ECAR that was acute and transient in nature (Fig. 1A). This is consistent with an acute increase of glycolytic flux by transient fuelling of glycogen-derived glucose units until glycogen was depleted. Interestingly, the transient change in ECAR was accompanied by a reciprocal, transient decrease in OCR (Fig. 1B).

After establishing ECAR as a proxy for glycogenolysis in the absence of glucose, we next examined the role of sAC-cAMP in glycogenolysis. Because sAC has a constitutive basal activity supported by intracellular ATP and bicarbonate, we examined the effect of the sAC-specific inhibitor LRE1 [46] on glycogenolysis in the absence of glucose. We validated the effect of sAC inhibition by LRE1 in HepG2 cells over-expressing the human truncated sAC isoform (htsAC) [9] (Fig. S1A-S1B) because the endogenous sAC activity in HepG2 is low. In H69 human cholangiocytes, which has a high sAC expression and activity [19,30], LRE1 also effectively inhibited cAMP accumulation (Fig. S1C). Surprisingly, when acutely inhibiting sAC-derived cAMP with the sAC-specific inhibitor LRE1, a transient increase in ECAR and a concomitant, reciprocal OCR transient were observed (Fig. 1C and D). The dynamic of ECAR transient induced by tmAC activation and sAC inhibition are also comparable. Calculation of the concomitant ATP production rates showed that ATP production by glycolysis was transiently stimulated upon sAC inhibition, while ATP production by TCA cycle and oxidative phosphorylation were transiently suppressed (Fig. S2A-D). During these transient changes in ECAR and OCAR, the overall ATP production (Fig. S2E) and the adenylate energy charge (Fig. S2F) remained constant.

Of note, under glucose starvation, sAC inhibition did not suppress FCCP-uncoupled OCR and only transiently suppressed coupled OCR as a response to increased ATP production by glycolysis (Fig. 1C and D), suggesting that sAC inhibition directly caused a transient increase in glycolytic flux during glucose deprivation. Indeed, when HepG2 cells were incubated in the presence of 2-deoxyglucose (2-DG, an inhibitor of glycolysis), the transients induced by sAC inhibition were abolished (Fig. 1E and F). The changes in ECAR and OCR induced by sAC inhibition were also largely prevented by co-incubation with CP-91149 (Fig. 1G and H), an established inhibitor for glycogen phosphorylase *a* [47], supporting that glycogen was the source for the glucose units used by the cells during glucose deprivation and sAC inhibition. Taken together, these results suggested that sAC-dependent cAMP signaling suppresses glycogen metabolism, which is opposite to the established glycogenolytic effect of tmAC-dependent cAMP signaling.

3.2. Inhibition of soluble adenylyl cyclase promotes glycogenolysis in various cell types

While liver and muscles are the primary organs for glycogen storage, glycogen can be detected in virtually all cells including tumor cell lines of various tissue origins [48]. Indeed, we found that HepG2 cells store significant quantities of glycogen which were, in the absence of added glucose, greatly reduced upon sAC inhibition as well as upon stimulation of tmACs with forskolin (Fig. 2A). The marked disappearance of glycogen under both conditions was, as expected, accompanied by a stimulation of lactate release (Fig. 2B). In contrast, sAC inhibition did not cause a strong decrease in the glycogen content of HepG2 cells in the presence of glucose (Fig. 2C). Furthermore, the glycogen phosphorylase *a* inhibitor CP-91149 strongly prevented glycogen breakdown induced by sAC inhibition in the absence of glucose (Fig. 2D).

We next confirmed the effect of pharmacological sAC inhibition by short hairpin RNA-mediated knockdown. Because sAC has multiple isoforms due to alternative splicing of the transcript, we selected 3 validated short hairpin RNA constructs (sACKD #128, #1280, #1388) to identify sAC proteins in HepG2 cells [19,30,45]. Immunoblotting showed that HepG2 cells expressed a 75 kD sAC isoform, which was effectively knocked down by short hairpin sACKD #128 and #1388 (Fig. 2E). We continued the metabolic studies with the short hairpin construct sACKD #1388, which targets the second catalytic domain of sAC [30,45]. Consistent with the previously reported role of sAC in regulation of cytosolic NADH/NAD^+ redox state, sACKD#1388 HepG2 cells showed elevated medium lactate-to-pyruvate ratios (Fig. 2F) [19]. In agreement with the pharmacological sAC inhibition, knockdown of sAC enhanced glycogen breakdown (Fig. 2G) and lactate secretion (Fig. 2H) in the absence of glucose. Like with pharmacological sAC inhibition, the glycogen phosphorylase *a* inhibitor CP-91149 also inhibited glycogen breakdown and lactate secretion induced by sAC knockdown. These data suggest that sAC inhibition promotes glycogen breakdown by increasing glycogen phosphorylase activity and that the presence of glucose allows cells to replete glycogen, thus preventing depletion of glycogen content upon sAC inhibition.

In the subsequent experiments, we investigated whether the glycogenolysis induced by sAC inhibition also occurred in other cell types. In primary mouse hepatocytes, inhibition of sAC caused glycogen breakdown both in the presence and absence of added glucose (Fig. 3A and B) and this glycogenolytic effect of sAC inhibition was, just as in HepG2 cells, sensitive for phosphorylase inhibition (Fig. 3B). To strengthen our findings, we examined if sAC also regulates glycogen metabolism in the immortalized human intrahepatic cholangiocytes H69 (hereafter H69 cholangiocytes), which have a high activity of sAC [30]. In H69 cholangiocytes, sAC inhibition caused net glycogen breakdown both in the presence and absence of extracellular glucose (Fig. 3C). Importantly, also in these cells, both stimulation of tmACs by forskolin and inhibition of sAC induced glycogen breakdown, demonstrating again the opposite effects of cAMP signaling by tmACs-derived cAMP and sAC-derived

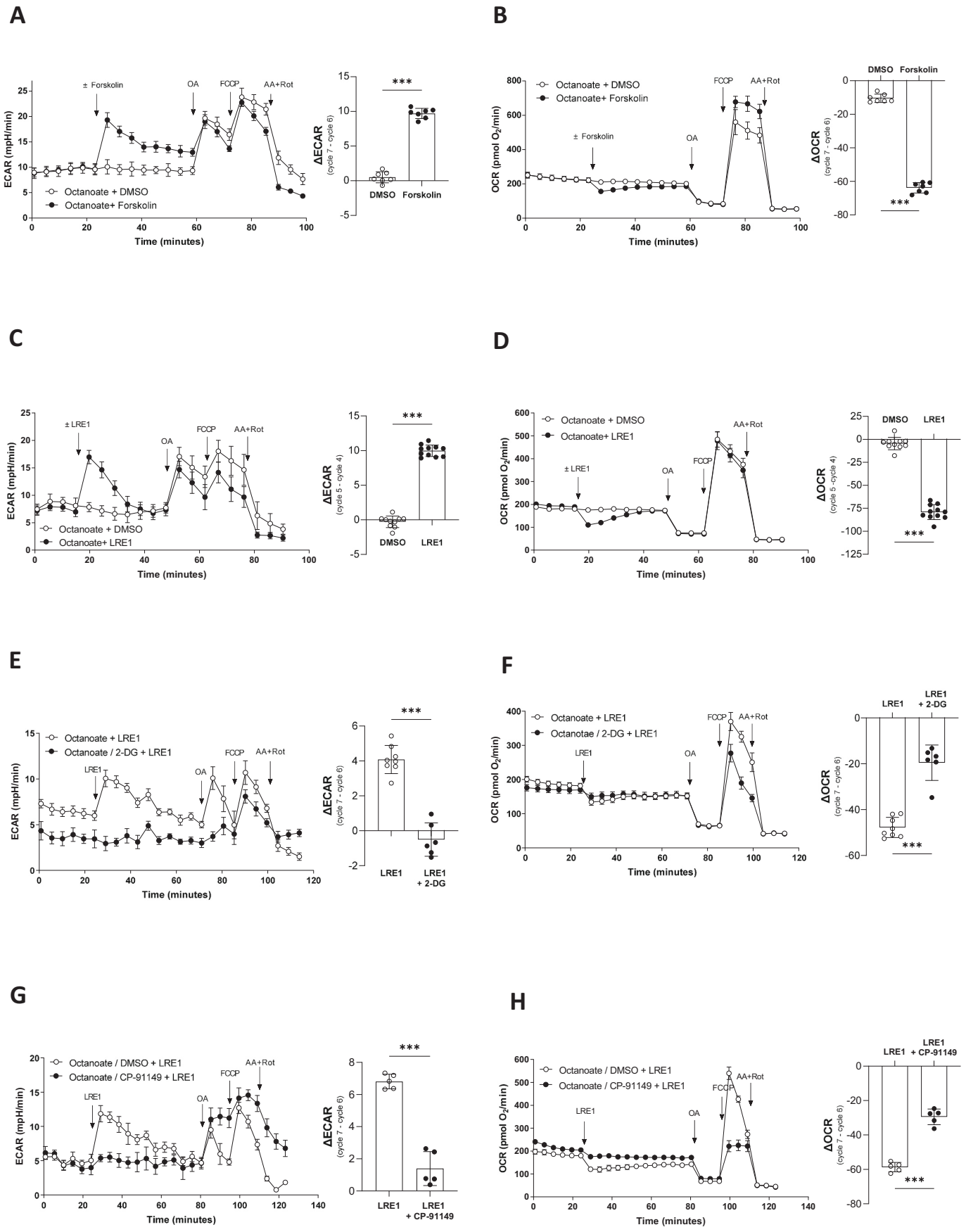

(caption on next page)

Fig. 1. Inhibition of soluble adenylyl cyclase causes transient changes in glycolysis and oxygen uptake in HepG2 cells.
HepG2 cells were preincubated for 1 h in HBSS for ambient air in the presence of 125 μM octanoate. The extracellular acidification rate (ECAR) and the oxygen consumption rate (OCR) were then analyzed by Seahorse Flux Analyzer XF96. Arrows indicate the injection of 0.1 % DMSO (vehicle control) or 1 μM forskolin (A-B) or 50 μM LRE1 (C-H). Subsequently, oligomycin A (OA), carbonyl cyanide-*p*-trifluoromethoxy-phenyl hydrazone (FCCP), and antimycin A (AA) and rotenone (Rot) were added as indicated in the figures. HepG2 cells were also tested in the presence of 5.5 mM 2-deoxyglucose (2-DG, E-F) or 100 μM CP-91149 (G-H). Data are presented as mean ± SD of at least 5 replicates for each condition. Statistical analysis: The maximal effects of forskolin (A-B) and sAC inhibitor LRE1 (C-H) on ECAR or coupled OCR were calculated as the differences of the ECAR or OCR values of the cycles before and after compound injection. Statistical analysis: Two-tailed unpaired Student's *t*-test. ***, $P < 0.001$. All data are representative of at least 3 independent experiments.

cAMP within the same cell (Fig. 3D). Taken together, these data indicate that sAC activity prevents depletion of glycogen.

3.3. sAC-derived cAMP and tmAC-derived cAMP engage different cAMP effectors to regulate glycogen homeostasis

We next investigated by which effector sAC-derived cAMP exerts its effect on glycogen. sAC-derived cAMP has been shown to signal via both Epac [49,50] and PKA [13,51]. In glucose-starved HepG2 cells that were fuelled with only octanoate, inhibition of Epac1 by the specific inhibitor (*R*)-CE3F4 [52] induced an acute, transient increase in ECAR with the same temporal and dynamic characteristics as sAC inhibition (Fig. 4A). In contrast, the PKA inhibitor H89 was without any effect. The Epac2-specific inhibitor ESI-05 [53] also did not induce changes in ECAR (Fig. 4A).

To corroborate the observed ECAR changes, we examined the effects of inhibition of Epac1, Epac2, and PKA on cellular glycogen levels. Indeed, in HepG2 cells acutely deprived of glucose, only inhibition of Epac1 phenocopied the glycogenolysis induced by sAC inhibition (Fig. 4B). In addition, the PKA-selective activator dibutyryl-cAMP promoted glycogen breakdown, confirming that PKA and Epac1 mediate opposite metabolic effects of tmAC and sAC signaling, respectively. A similar result was obtained in H69 cholangiocytes incubated without glucose (Fig. 4C). Moreover, we observed that in the presence of glucose, the Epac1-specific inhibitor (*R*)-CE3F4 induced significant glycogen breakdown in H69 cholangiocytes but not in HepG2 cells (Fig. 4D and E), which mirrored the differential effects of sAC inhibition on glycogen breakdown in these cells. Of note, inhibition of sAC or Epac1 also induced glycogenolysis and the concomitant release of lactate in several other cell lines in the absence of glucose (Fig. S3A-S3D). Taken together, our data suggest that Epac1 mediates the sAC-dependent repression of glycogenolysis in several cell types, whereas tmAC-activated PKA oppositely induces glycogenolysis.

3.4. Glucose deprivation reveals a complex I-independent regulation of glycogenolysis by sAC

We and others have shown that sAC regulates the activity of complex I of the mitochondrial respiratory chain [19,51,54]. Inhibition of complex I can reduce the steady state glycogen levels via AMPK-dependent suppression of glycogen synthase activity [55–57]. Indeed, in cultured primary murine astrocytes, sAC inhibition suppresses oxidative phosphorylation, leading to AMPK activation and a decrease in glycogen level [36]. However, because sAC inhibition also induces glycogen breakdown in the absence of glucose (Figs. 1 and 2), leaving glycogen synthase without substrate, we examined whether the induction of glycogenolysis upon sAC inhibition was mediated by complex I suppression or by another, yet unknown, mechanism. To this end, we examined whether the complex I inhibitor rotenone could phenocopy the metabolic effects of sAC inhibition. In glucose-fed HepG2 cells, 15 nM rotenone suppressed coupled OCR to a comparable extent as 50 μM LRE1 (Fig. 5A). However, in the absence of glucose, rotenone caused a much smaller ECAR transient than LRE1 (Fig. 5B). Rotenone had also a much smaller effect on lactate release under these conditions (Fig. 5C). Although the addition of rotenone to HepG2 cells did result in clear AMPK activation even to a greater extent than LRE1 did (Fig. S4), this dose of rotenone did not induce significant glycogen breakdown (Fig. 5D). Thus, these data strongly suggest that sAC regulates glycogenolysis independently of its regulation of complex I.

3.5. Activation of glycogen phosphorylase a by sAC-cAMP-Epac1 signaling

Finally, we sought to characterize how sAC regulates glycogenolysis in the presence of a physiological concentration of glucose (5.5 mM). The glycogen content of cells depends on the balance between glycogen synthase activity and glycogen phosphorylase activity. Since the inhibition of sAC-cAMP-Epac1 signaling promoted glycogenolysis in the absence of glucose, leaving glycogen synthase without substrate, we anticipated that inhibition of sAC-cAMP-Epac1 signaling promotes glycogen breakdown by promoting the conversion of glycogen phosphorylase from the inactive “T state” to the active “R state”. This T-to-R conversion is stimulated by phosphorylase kinase-mediated phosphorylation of the Ser-15 residue of glycogen phosphorylase [34,58,59]. In the presence of glucose, both the sAC-specific inhibitor LRE1 and the tmAC-specific activator forskolin increased Ser-15 phosphorylation of glycogen phosphorylase (PYGL) in HepG2 cells (Fig. 6A), albeit with a kinetics slower than that of the ECAR increase observed in the absence of glucose (Fig. 1C). Of note, rotenone did no induced significantly Ser-15 phosphorylation in HepG2 cells as compared to the DMSO control (Fig. 6A). Late changes in phosphorylase phosphorylation in HepG2 cells were also induced by the Epac1 inhibitor (*R*)-CE3F4 (Fig. 6B). In H69 human cholangiocytes, sAC or Epac1 inhibition induced an early increase in phosphorylase phosphorylation (Fig. 6C and D). These observations support that sAC-cAMP-Epac1 signaling also regulates glycogen breakdown in the presence of glucose.

4. Discussion

Our present study shows that sAC-mediated regulation of glycogen breakdown occurs by a completely novel sAC-cAMP-Epac1 signaling pathway, which operates in an opposite way compared to the canonical tmAC-cAMP-PKA signaling. The current evidence support that cAMP signaling operates in compartmentalized micro- or nano-domains [7,20,22] with the spatial specificity governed by several mechanisms, including buffering by regulatory units of PKA [23], degradation by phosphodiesterases (PDEs) [24,25], scaffolding proteins [28,60], and cAMP-impermeable membranes such as the mitochondrial inner membrane [16]. Our findings show that, despite both engaging the cAMP signaling in the cytosol, sAC-derived cAMP suppresses glycogen breakdown by engaging cAMP effector Epac1 while the tmAC-derived cAMP engages PKA to stimulate glycogen breakdown. Our findings thus support that the specificity of cAMP signaling can also be maintained at the level of cAMP effectors. In line with this reasoning, tmAC-derived cAMP engages PKA to suppress protein kinase B (PKB/Akt) activation, but promotes PKB/Akt activation when engaging Epac1 [61].

4.1. sAC-cAMP-Epac1 signaling as a novel mechanism to regulate glycogen metabolism for autonomous energy homeostasis in cells

Glycogen, albeit often at a lower level than the specialized glycogen-storing tissues (i.e. the liver and muscles), is also normally present in non-specialized tissues or accumulates in some pathologic conditions (e.g. brain [62,63], kidney [64], heart [65], adipose tissues [66,67],

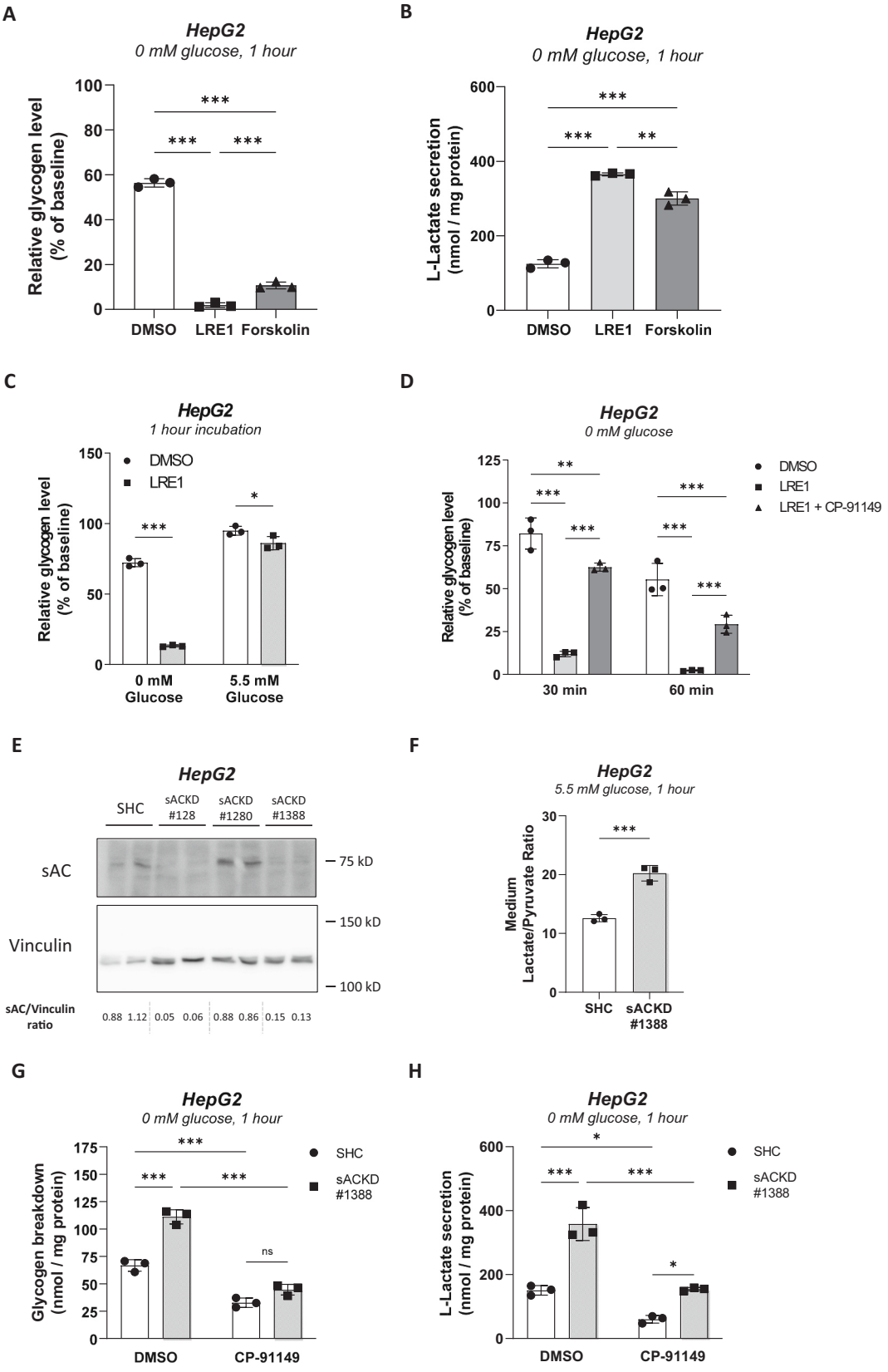

(caption on next page)

Fig. 2. Inhibition of soluble adenylyl cyclase promotes glycogenolysis in HepG2 cells.
(A) HepG2 cells were pre-incubated with 5.5 mM glucose for 1 h. After harvesting baseline samples, cells were incubated with medium without glucose in the presence of 0.1 % DMSO (vehicle control), 50 μM LRE1 or 1 μM forskolin for another hour and then harvested for glycogen determination. Data were expressed as % of the baseline value (154 ± 21 nmol glucosyl unit per mg protein, $n = 6$) and mean ± SD. (B) HepG2 cells were treated exactly as described under (A) and the lactate concentration in the medium was determined in samples taken after 60 min of incubation. Data represent mean ± SD of triplicate samples. Results shown are representative of 2 independent experiments. (C) HepG2 cells were pre-incubated with 5.5 mM glucose for 1 h. After harvesting baseline samples, cells were refreshed with medium ± 5.5 mM glucose ± 50 μM LRE1 for another hour and then harvested for glycogen determination. Data were expressed as % of the baseline value (231 ± 22 nmol glucosyl unit per mg protein, $n = 3$) and mean ± SD. (D) HepG2 cells were pre-incubated with 5.5 mM glucose for 1 h. After harvesting the baseline samples, cells were exposed to media without glucose in the presence of 0.1 % DMSO, 50 μM LRE1, or 50 μM LRE1 + 100 μM CP-91149. Glycogen content was determined after 30 and 60 min of incubation. Data are expressed as % of the baseline value (119 ± 2 nmol glucosyl unit per mg protein, $n = 4$) and mean ± SD. (E) HepG2 cells were acutely transduced with lentiviruses carrying the control short hairpin (SHC) or sAC knockdown short hairpin constructs (sACKD #128, #1280, #1388). The efficiency of sAC knockdown was evaluated by immunoblotting. Data represent two independent lentiviral transductions. (F) HepG2 cells were acutely transduced with lentivirus carrying the control short hairpin (SHC) or the sACKD short hairpin #1388. Two days after lentiviral transduction, medium lactate-to-pyruvate ratios were determined in the presence of 5.5 mM glucose. Data from three independent experiments are expressed as mean ± SD. (G-H) HepG2 cells were transduced with lentiviruses carrying the control short hairpin (SHC) or the sACKD hairpin #1388. Cells were pre-incubated with 5.5 mM glucose for 1 h and the medium was acutely switched to the glucose-free medium in the presence and absence of 30 μM CP-91149 for 1 h to determine glycogen breakdown. The reduction of glycogen levels in cells (G) and the secretion of L-lactate (H) was normalized to protein content. Data from three independent experiments are expressed as mean ± SD. Statistical analysis: (A-B) One-way ANOVA with Tukey's multiple comparisons test. (C-D) Two-way ANOVA with Šídák's multiple comparisons test. (E) Two-tailed unpaired Student's *t*-test. (G-H) Two-way ANOVA with Tukey's multiple comparisons test. ***, $P < 0.001$; **, $P < 0.002$; *, $P < 0.033$.

macrophages [68], and tumor cells of various tissue origins [48]). The glycogen store in the non-specialized tissues likely supports certain tissue-specific functions. For instance, the glycogen store of astrocytes can serve as an emergency energy source for neurons in the brain and is critical for learning and memory [69,70]. Although also equipped with the enzymatic machinery for glycogen metabolism (e.g. glycogen phosphorylase and glycogen synthase), non-specialized tissues in general do not express the GPCRs (e.g. glucagon receptor) necessary to engage the canonical glucagon regulation by the tmAC-cAMP-PKA signaling. This implies that other mechanisms exist in these cells to regulate the metabolism of glycogen. Our present study shows that sAC regulates glycogenolysis via a novel sAC-cAMP-Epac1 signaling pathway that suppresses glycogen breakdown in cells of both specialized and non-specialized tissue origins, including liver, kidney, breast, and intestines. Because sAC is not regulated by GPCR or G proteins, is expressed in most tissues, and functions as an evolutionarily conserved metabolic sensor for ATP (due to high K_m for ATP) and Krebs cycle activity (via bicarbonate, derived from CO_2 of Krebs cycle) [6,11,13], the sAC-cAMP-Epac1 signaling likely represents a regulatory mechanism to use glycogen stores to maintain autonomous energy homeostasis in cells. Under well-fed conditions, sufficient ATP and Krebs cycle activity is sensed by sAC and the sAC-cAMP-Epac1 signaling prevents unnecessary breakdown of glycogen. On the other hand, when cells are starved of nutrients or oxygen, low cellular ATP or Krebs cycle activity decreases sAC activity, leading to enhanced glycogen breakdown for ATP generation. Importantly, we found that under glucose starvation, sAC inhibition did not reduce FCCP-uncoupled, indicating that the transient OCR suppression is a secondary response to an increased ATP production from glycogen breakdown and glycolysis (Figs. 1 and S2). The regulation of glycogen breakdown in glucose-starved conditions (this study) and the regulation of the switch between glycolysis and oxidative phosphorylation in glucose-sufficient conditions [19] by sAC-cAMP-Epac1 signaling together support that sAC is a metabolic sensor and regulator of autonomous energy homeostasis in cells.

4.2. How sAC-cAMP-Epac1 signaling regulates glycogen breakdown

In this study, we showed that suppression of sAC-cAMP-Epac1 leads to Ser-15 phosphorylation of the liver-form glycogen phosphorylase (PYGL) as a mechanism of glycogen breakdown (Fig. 7). The Ser-15 residue of PYGL is the primary phosphorylation site of phosphorylase kinase and is present in all three mammalian glycogen phosphorylase isoforms: the liver-form (encoded by *PYGL*), the muscle form (encoded by *PYGM*), and the brain-form (encoded by *PYGB*). Expression data from the Human Protein Atlas showed that the cell lines used in this study (HepG2, Caco-2, HEK293, and HeLa) express both the liver-form and the brain-form glycogen phosphorylase, but not the muscle-form phosphorylase (Supplementary Fig. S5A) [71]. However, because the activity of the muscle-form and the brain-form glycogen phosphorylases is also increased upon Ser-15 phosphorylation by phosphorylase kinase, sAC-cAMP-Epac1 signaling is also expected to regulate the glycogen metabolism in tissues expressing the muscle-form or the brain-form glycogen phosphorylases. Ser-15 phosphorylation of glycogen phosphorylases is regulated by the cyclic cascade of phosphorylase kinase and phosphoprotein phosphatase 1 (PP-1). In HepG2 cells, when inhibiting PP-1 with okadaic acid, we did not observe any ECAR transient as seen with sAC or Epac1 inhibition (data not shown), indicating that sAC-cAMP-Epac1 signaling does not increase Ser-15 phosphorylation of glycogen phosphorylase via inhibition of PP-1. Therefore, suppression of sAC-cAMP-Epac1 signaling most likely leads to activation of phosphorylase kinase.

How Epac1 inhibition leads to activation of phosphorylase kinase would require further studies and we can only speculate the possible mechanism here. Phosphorylase kinase is a 1300 kDa oligomer ($\alpha_4\beta_4\gamma_4\delta_4$) made from four different subunits and operates by the "disinhibition-activation mechanism" [72]. The γ-subunit of phosphorylase kinase is the catalytic subunit and is inherently active. The α-, β-, and δ-subunits are regulatory subunits and suppress the activity of γ-subunit in the oligomerized state. The δ-subunit is identical to calmodulin. The expression levels of individual subunits in cell lines used in this study and reference cell types are summarized in Supplementary Fig. S5B-S5E. Epac1 has been shown to form a complex with and activate calmodulin-dependent protein kinases (CaMKII) in mitochondria [73,74] and at the plasma membrane [75]. It is unknown if Rap1 activation by Epac1 is required for forming the Epac1-CaMKII complex, but indirect evidence suggests that Rap1 interacts with calmodulin [76]. Importantly, both genetic and pharmacological suppression of CaMKII leads to increased cytosolic free [Ca^{2+}], which can activate phosphorylase kinase [77,78]. Moreover, on sarcoplasmic reticulum, CaMKII was reported to assemble a glycolytic enzyme complex consisting of phosphorylase kinase, aldolase A, glyceraldhyde-3-phosphate dehydrogenase, enolase, pyruvate kinase, and lactate dehydrogenase [79]. Based on the interactions between Epac1, CaMKII and phosphorylase kinase, we speculate that the suppression of sAC-cAMP-Epac1 signaling could inhibit CaMKII and increase basal free [Ca^{2+}] in the cytosol to activate phosphorylase kinase via its δ-subunits (calmodulin). This would constitute a mechanism that operates independently of the tmAC-cAMP-PKA signaling, which activate the phosphorylase kinase by phosphorylating the α- and β-subunits.

Another possible mechanism for Epac1 signaling to regulate glycogen metabolism is through Rap1-dependent activation of mTOR (mammalian target of rapamycin) complex 1 (mTORC1) [80,81]. In tuberous sclerosis complex (TSC), loss-of-function mutations in TSC1 or TSC2 cause hyperactivation of mTORC1, which causes pathologic

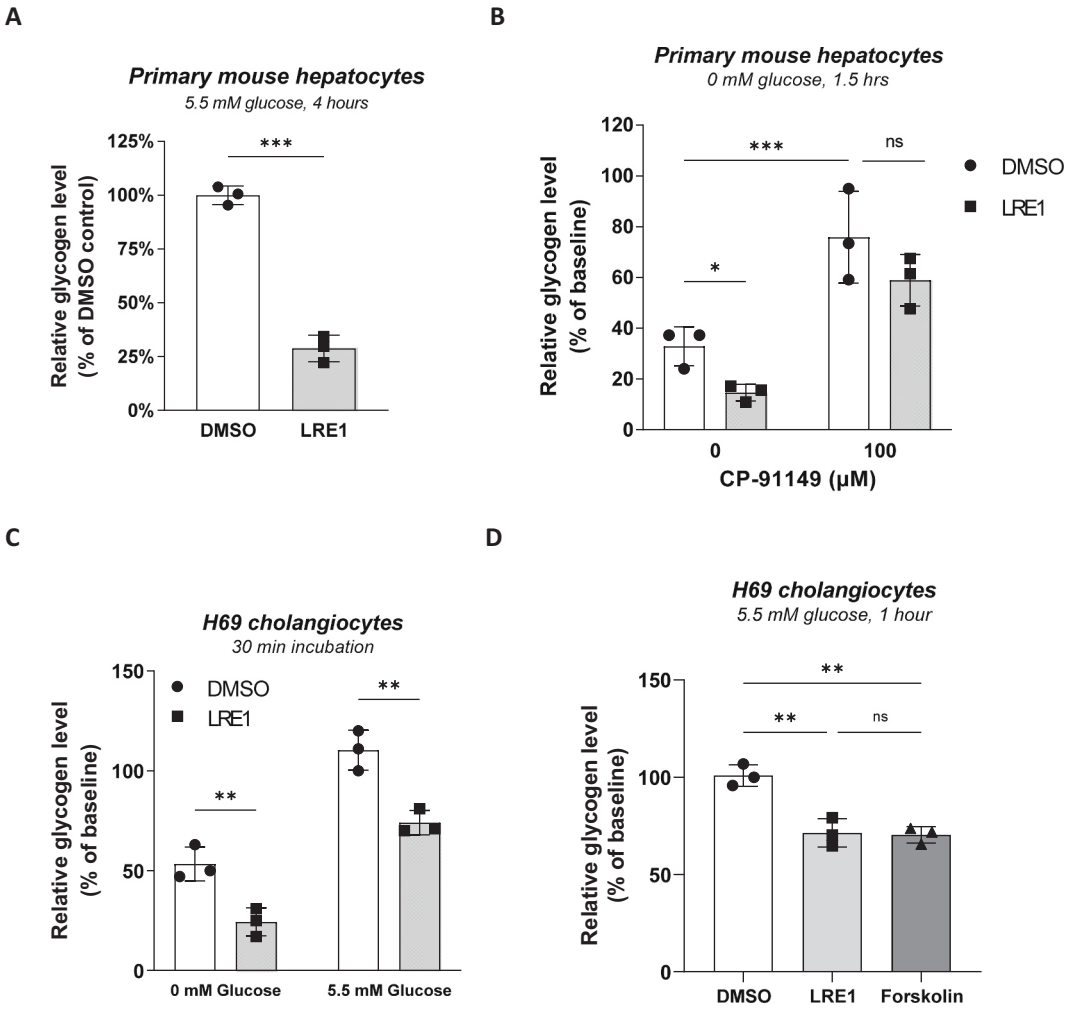

Fig. 3. Effects of sAC inhibition on glycogen levels in primary mouse hepatocytes and H69 cholangiocytes.
(A) Primary mouse hepatocytes were incubated in the presence of 5.5 mM glucose for 4 h with 50 μM LRE1 or 0.1 % DMSO (vehicle control). Glycogen content was determined and normalized to protein content. Data are expressed as % of the vehicle control value (132 ± 6 nmol glucosyl unit per mg protein, n = 3) and mean ± SD of triplicate determinations. (B) Primary mouse hepatocytes were acutely starved of glucose in the presence or absence of 50 μM LRE1 and 100 μM CP-91149 for 1.5 h. Glycogen content was determined and normalized to protein content. Data are expressed as % of the baseline value (224 ± 16 nmol glucosyl unit per mg protein, n = 3) and mean ± SD. (C) H69 cholangiocytes were preincubated with 5.5 mM glucose for 1 h. After harvesting baseline samples, cells were incubated with medium ± 5.5 mM glucose ± 50 μM LRE1 for 30 min and then harvested for glycogen determination Data are expressed as % of the baseline value (52 ± 3 nmol glucosyl unit per mg protein, n = 3) and mean ± SD. (D) H69 cholangiocytes were pre-incubated with 5.5 mM glucose for 1 h. After harvesting baseline samples, the incubations were continued in the presence of 0.1 % DMSO (vehicle control), 50 μM LRE1, or 1 μM forskolin for 1 h. Glycogen content was determined and normalized to protein content. Data are expressed as % of the baseline value (213 ± 8 nmol glucosyl unit per mg protein, n = 3) and mean ± SD. All data are representative of 2–3 independent experiments. Statistical analysis: (A) Two-tailed unpaired Student's *t*-test (B) Two-way ANOVA with Dunnett's multiple comparisons test. (C) Two-way ANOVA with Šídák's multiple comparisons test. (D) One-way ANOVA with Šídák's multiple comparisons test. ***, $P < 0.001$; **, $P < 0.002$; *, $P < 0.033$; ns, not significant.

glycogen accumulation in tissues [82,83]. It is therefore possible that under nutrient-sufficient conditions, sAC-cAMP-Epac1-Rap1 signaling can maintain the glycogen store via mTORC1 activity.

4.3. Secondary mechanisms in sAC-cAMP-Epac1-mediated glycogen regulation

The activity of phosphorylase kinase is highly pH-dependent, with the activity at pH 8.2 being 14- to 25-fold higher than at pH 6.8 [84,85]. Therefore, the ECAR transient (i.e. transient increase in proton efflux) can in theory cause a reciprocal intracellular alkalinization to stimulate phosphorylase kinase activity and glycogen breakdown. The increased glycolytic flux from glycogen breakdown can lead to further extracellular acidification and reciprocal intracellular alkalinization, forming a positive feedback loop to drive further glycogen breakdown. Consistently, we observed that the kinetics of Ser-15 phosphorylation of glycogen phosphorylase upon suppression of sAC-cAMP-Epac1 signaling (Fig. 6) lags behind the kinetics of the ECAR transient (Figs. 1 and 4).

Phosphorylase kinase is allosterically stimulated by ADP [86] and glycogen phosphorylase is allosterically activated by AMP [58]. sAC-cAMP signaling has been shown by us and others to regulate Complex I and complex IV of the mitochondrial electron transport chain by PKA or Epac1 [13,19,46,51]. Therefore, a decrease in sAC activity can also regulate glycogen metabolism via secondary changes in the adenylate nucleotides. Although we did not observed changes in total ATP production rates and adenylate energy charges by sAC inhibition (Fig. S2), sAC inhibition did however increase AMPK activity as shown by increased ACC phosphorylation (Fig. S4). Therefore, acute sAC inhibition likely caused a transient elevation of cytosolic [ADP]/[ATP] and [AMP]/[ATP] ratios, which, although rapidly rectified, might be sufficient to allosterically activate AMPK, phosphorylase kinase and glycogen phosphorylase. Similarly, Jakobsen et al. also reported

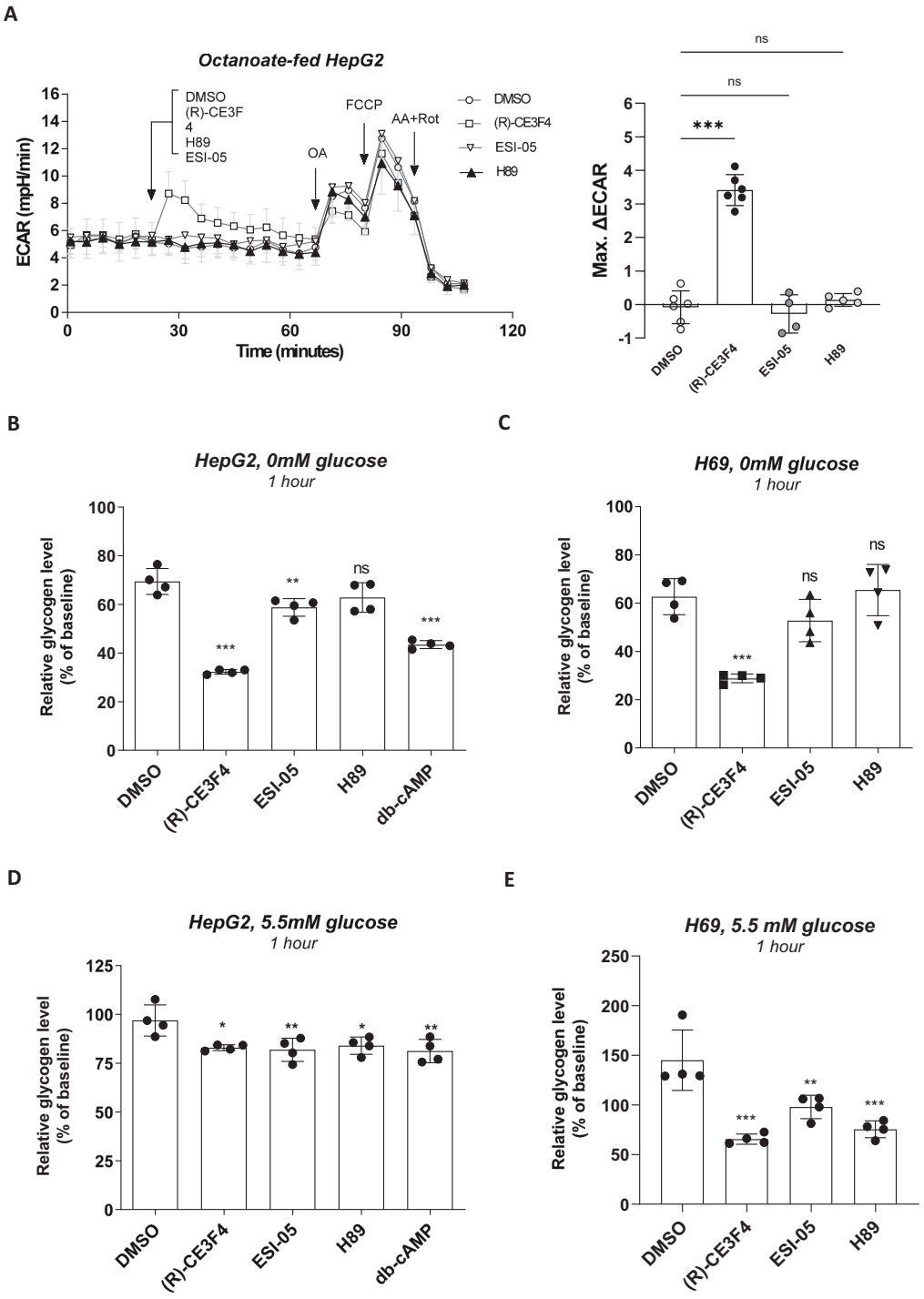

Fig. 4. sAC-derived and tmAC-derived cAMP engage different cAMP effectors to regulate glycogen breakdown.
(A) HepG2 cells were pre-incubated for 1 h in HBSS for ambient air with 125 μM octanoate and then the extracellular acidification rate (ECAR) was measured with the Seahorse Flux Analyzer XF96. After the baseline measurement, 0.1 % DMSO (vehicle control, $n = 6$), 50 μM (*R*)-CE3F4 (n = 6), 10 μM ESI-05 (n = 4) or 10 μM H89 ($n = 5$) was injected, followed by oligomycin A (OA), carbonyl cyanide-p-trifluoromethoxy-phenyl hydrazone (FCCP), and antimycin A (AA) and rotenone (Rot). Data are presented as mean ± SD. (B-C) HepG2 cells (B) and H69 cholangiocytes (C) were acutely incubated in glucose-free medium for 60 min in the presence of 0.1 % DMSO (vehicle control), 50 μM (*R*)-CE3F4, 10 μM ESI-05, or 10 μM H89. HepG2 cells were also treated with 100 μM dibutyryl-cAMP (db-cAMP) as positive control. Glycogen content was determined and normalized to protein content. Data are expressed as % of the baseline value (HepG2: 71 ± 3 nmol glucosyl unit per mg protein, $n = 4$. H69: 130 ± 13 nmol glucosyl unit per mg protein, n = 4) and mean ± SD. (D-E) HepG2 cells (D) and H69 cholangiocytes (E) were incubated in the experimental medium containing 5.5 mM glucose for 1 h in the presence of 0.1 % DMSO (vehicle control), 50 μM (*R*)-CE3F4, 10 μM ESI-05, or 10 μM H89. HepG2 cells were also treated with 100 μM dibutyryl-cAMP (db-cAMP) as positive control. Glycogen content was determined and normalized to protein content. Data are expressed as % of the baseline value (HepG2: 74 ± 2 nmol glucosyl unit per mg protein, n = 4. H69: 147 ± 9 nmol glucosyl unit per mg protein, n = 4) and mean ± SD. All data are representative of 2–3 independent experiments. Statistical analysis: (A) The maximal effects of DMSO, (*R*)-CE4F4, ESI-05, H89 on ECAR were calculated as the differences of the ECAR values of the cycles before and after compound injection. Two-tailed unpaired Student's *t*-test. (B-E) One-way ANOVA with the Dunnett's multiple comparisons test (compared to DMSO). ***, $P < 0.001$; **, $P < 0.002$; *, $P < 0.033$; ns, not significant.

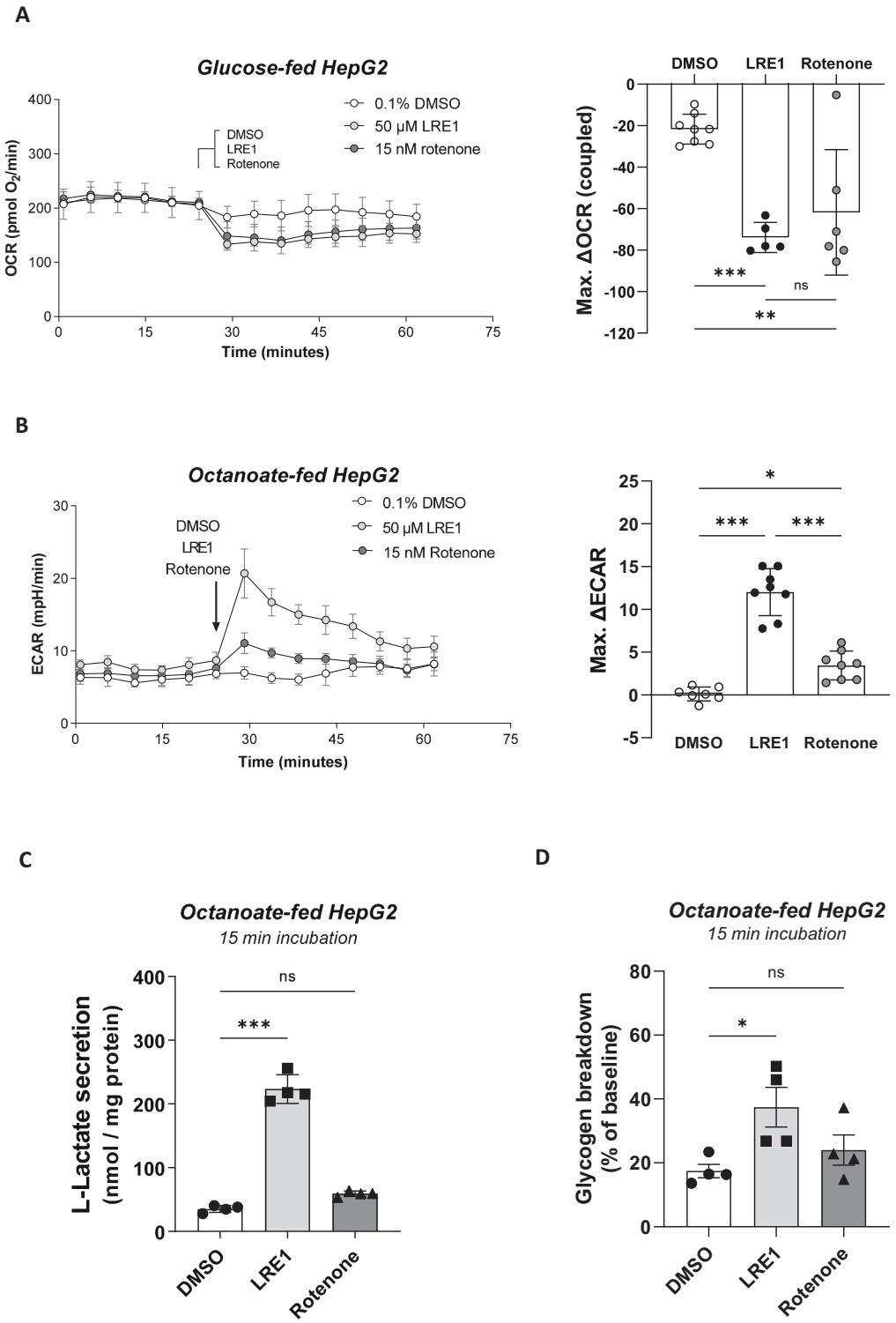

Fig. 5. sAC regulates glycogen breakdown independently of complex I inhibition.
(A) HepG2 cells were pre-incubated in HBSS for ambient air in the presence of 5.5 mM glucose for 30 min and then the oxygen consumption rate (OCR) was measured with the Seahorse Flux Analyzer XF96. After baseline measurement, 0.1 % DMSO (vehicle control, $n = 8$), 50 μM LRE1 (n = 5) or 15 nM rotenone (n = 6) was injected. (B) HepG2 cells were pre-incubated in HBSS for ambient air in the presence of 125 μM octanoate for 30 min and then the oxygen consumption rate (ECAR) was measured with the Seahorse Flux Analyzer XF96. After baseline measurement, 0.1 % DMSO (vehicle control, n = 6), 50 μM LRE1 (n = 6) or 15 nM rotenone (n = 6) was injected. (C-D) HepG2 cells were pre-incubated in glucose-free HBSS with 125 μM octanoate for 30 min and then the medium was replaced by the same incubation medium containing 0.1 % DMSO (vehicle control), 50 μM LRE1 or 15 nM rotenone. After 15 min of incubation, samples were taken from the extracellular medium to determine lactate release (C) and cell lysates were prepared to determine cellular glycogen levels (D). Data are presented as mean ± SD of quadruplicate determination. Statistical analysis: (A-B) The maximal effects of the treatment on coupled OCR or ECAR were calculated as the differences of the OCR or ECAR values of the cycles before and after compound injection. Two-tailed unpaired Student's *t*-test. (C) One-way ANOVA with Tukey's multiple comparisons test. (D) ***, $P < 0.001$; **, $P < 0.002$; *, $P < 0.033$; ns, not significant.

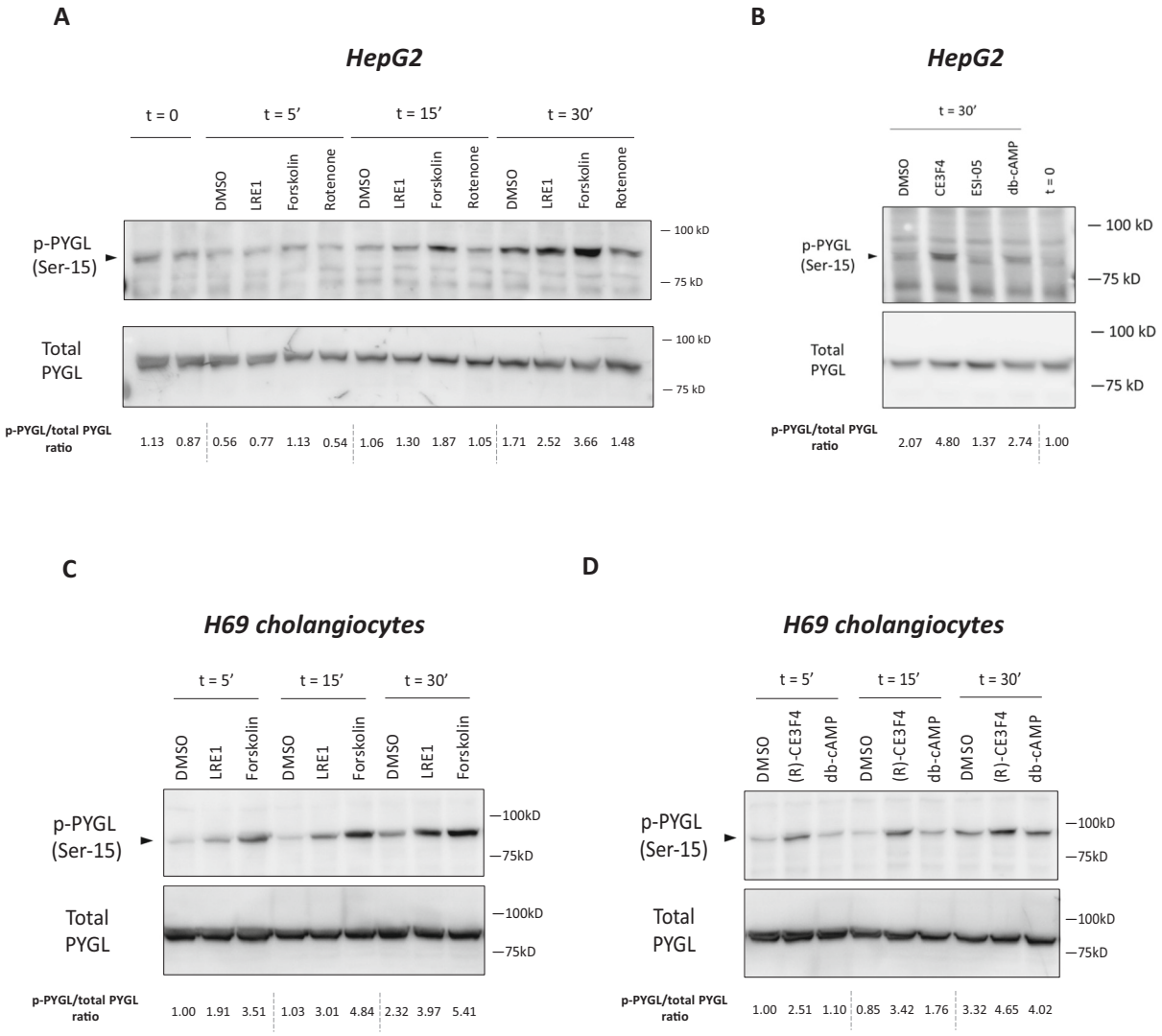

Fig. 6. Inhibition of sAC-cAMP-Epac1 signaling leads to activation of glycogen phosphorylase.
(A) HepG2 cells were incubated in serum-free DMEM containing 5.5 mM glucose for 1 h. Cells were then treated with 0.1 % DMSO (vehicle control), 50 μM LRE1, 1 μM forskolin, or 15 nM rotenone for 5, 15, and 30 min. Phosphorylation of Ser-15 of liver form glycogen phosphorylase (PYGL) was examined in cell lysates by immunoblotting. (B) HepG2 cells were incubated as in (A) but treated with 50 μM (*R*)-CE3F4, 10 μM ESI-05, or 100 μM db-cAMP for 30 min. Phosphorylation of Ser-15 of liver form glycogen phosphorylase (PYGL) was examined by immunoblotting. (C) H69 cholangiocytes were incubated under the same conditions as described in (A) and then challenged with 0.1 % DMSO (vehicle control), 50 μM LRE1 or 1 μM forskolin for the time periods indicated. Phosphorylation of PYGL was determined in cell lysates. (D) H69 cholangiocytes were incubated as described in (C) and then treated with 0.1 % DMSO (vehicle control), 50 μM (*R*)-CE3F4, or 100 μM db-cAMP for 30 min. Phosphorylated PYGL (p-PYGL) and total PYGL signals were quantified by densitometry and the p-PYGL/total PYGL ratio were calculated and normalized to the baseline ($t = 0$) sample(s) (A and B) or the DMSO control at t = 5′ (C and D). Results shown are representative of 2–3 independent experiments.

increased AMPK activity and concomitant glycogen breakdown in murine astrocytes following acute sAC inhibition [36].

4.4. Role of AMPK in sAC-cAMP-Epac1-dependent regulation of glycogen breakdown

The exact contribution of AMPK activation to glycogen breakdown by sAC inhibition would depend on the availability of extracellular glucose and the downstream effectors of AMPK in individual cell types. AMPK has been shown to phosphorylate glycogen synthase at the Ser-7 residue, which suppresses glycogen synthase activity by increasing its K_m for UDP-glucose (the substrate) and glucose-6-phosphate (G6P, an allosteric activator) [56,57]. It should be noted however that the same Ser-7 site is also phosphorylated by PKA, phosphorylase kinase, and glycogen synthase kinase 3 [56,87]. On the other hand, phospho-peptide analysis revealed no stoichiometric phosphorylation of glycogen phosphorylase by AMPK [56]. In the absence of extracellular glucose (Fig. 7A), glycogen synthase is essentially inactive due to very low levels of intracellular UDP-glucose and glucose-6-phosphate. Therefore, although AMPK-dependent phosphorylation of glycogen synthase can further suppress glycogen synthase activity, the added effect is likely limited. Consistently, In HepG2 cells, activation of AMPK by rotenone treatment also did not result in increased Ser-15 phosphorylation of PYGL and induced a much smaller glycogen degradation compared to sAC or Epac1 inhibition (Figs. S4, 5 and 6A). Taken together, AMPK activation is unlikely to be a primary mechanism of glycogen breakdown induced by sAC or Epac1 inhibition in the absence of glucose.

In the presence of extracellular glucose (Fig. 7B), glycogen synthase activity is high and AMPK activation can indeed lower glycogen synthase activity by phosphorylation; if phosphorylase is also activated at the same time, AMPK can potentiate net glycogen breakdown by reducing the “recycling” of glucose-1-phosphate derived from glycogenolysis. However, AMPK activation also increases glucose transporter 1 (GLUT1) levels at the plasma membrane to facilitate glucose uptake

A ***Without extracellular glucose***

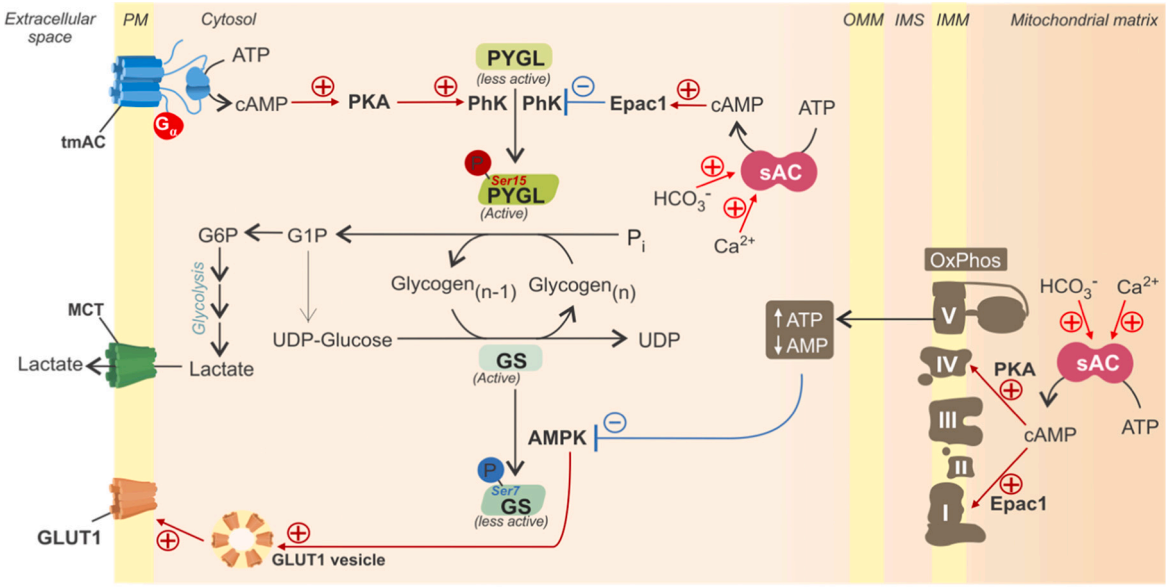

B ***With extracellular glucose***

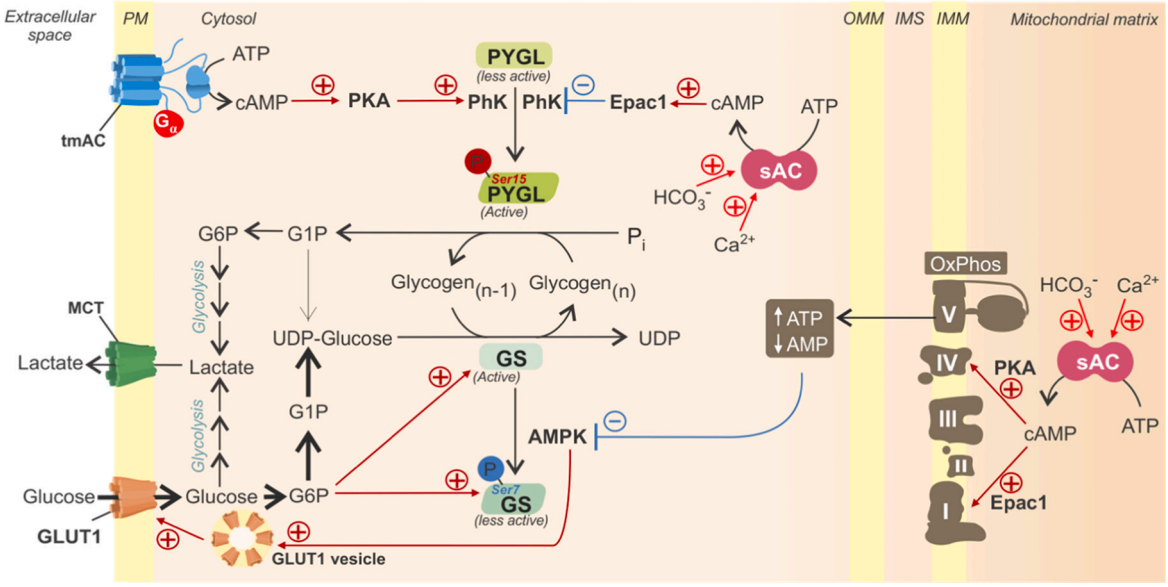

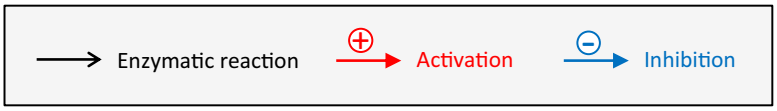

(caption on next page)

Fig. 7. Working models of how sAC regulates glycogen metabolism.
Binding of epinephrine or glucagon to their cognate G-protein-coupled receptors at the plasma membrane (not shown) releases the α-subunit (G_α) of the heterotrimeric G-protein, which activates the transmembrane adenylyl cyclases (tmACs). The canonical tmAC-cAMP-PKA signaling leads to glycogen breakdown by a phosphorylation cascade that activates phosphorylase kinase (PhK) and glycogen phosphorylase (PYGL, $pSer^{15}$). In contrast, soluble adenylyl cyclase (sAC) activity is not regulated by G-proteins, but is maintained by bicarbonate, Ca^{2+}, and ATP. The novel sAC-cAMP-Epac1 signaling operates oppositely to the tmAC-cAMP-PKA signaling and suppresses glycogen breakdown. (A) In the absence of glucose, inhibition of the sAC-cAMP-Epac1 signaling leads to activation of glycogen phosphorylase by Ser-15 phosphorylation, resulting in glycogen breakdown. Note that the inhibition of sAC-cAMP-Epac1 signaling also activates AMP-activated protein kinase (AMPK) due to suppression of complex I activity in mitochondria. AMPK can phosphorylate glycogen synthase (GS) at the Ser-7 residue to reduce GS activity, although the GS activity is already low due to low levels of glucose-6-phosphate (G6P) and UDP-glucose in the absence of glucose. (B) In the presence of glucose, inhibition of sAC-cAMP-Epac1 signaling also leads to increased PYGL activity and reduced GS activity. However, the activation of AMPK can increase glucose influx by increasing glucose transporter 1 (GLUT1) at the plasma membrane; the resulting rise in G6P and UDP-glucose levels can counteract GS inhibition by Ser-7 phosphorylation to prevent glycogen depletion. In the presence of glucose, the effect of sAC-cAMP-Epac1 inhibition on the steady state glycogen level depends on the balance of the overall activity of glycogen breakdown and synthesis. The models presented in 7A and 7B represent two extremes of glucose availability in pathophysiology. Abbreviation: PM, plasma membrane; OMM, outer mitochondrial membrane; IMS, intermembrane space of mitochondria; IMM, inner mitochondrial membrane; OxPhos, oxidative phosphorylation; PKA, protein kinase A; Epac1, exchange factor directly activated by cAMP 1; MCT, monocarboxylate transporter.

[88,89]. Thus, depending on the glucose influx and the resulting increase in intracellular G6P and UDP-glucose levels, allosteric activation and high substrate availability could overcome the covalent suppression of Ser-7 phosphorylation, which does not affect the V_{max} of glycogen synthase [57]. Indeed, pharmacological AMPK activation and constitutive AMPK activation due to mutations in *PRKAG2* both increase muscle glycogen levels *in vivo* and *ex vivo* [90–93]. Thus, in the presence of glucose, the balance of AMPK-dependent suppression of glycogen synthase, AMPK-induced glucose uptake via GLUT1, and the expression level of glycogen synthase decides the glycogen synthesis rate, which counteracts the increased glycogen breakdown rate induced by inhibiting sAC. The differences in glycogen synthesis rates likely explain why, in the presence of glucose, sAC inhibition remained effective in reducing the glycogen level in H69 cholangiocytes (Fig. 3C) but had a much smaller effect on HepG2 cells (Fig. 2C).

4.5. sAC-cAMP-Epac1 signaling as a potential therapeutic target to reverse pathologic glycogen accumulation

Pathologic glycogen accumulation impairs cellular and organ functions and is responsible for key disease manifestations in several genetic and hereditary diseases. In glycogen storage disease, pathological glycogen accumulation can occur in liver, skeletal muscle, and cardiac muscle, leukocytes, and fibroblasts, depending on the underlying genetic mutation [94,95]. In Lafora disease, loss-of-function mutations of laforin (a glucan phosphatase, encoded by *EPM2A*) or malin (an E3 ubiquitin ligase, encoded by *NHLRC1*) leads to accumulation of structurally abnormal, insoluble glycogen molecules in brain tissues, leading to progressive, intractable seizure attacks [96]. Currently, there are no pharmacotherapies to reduce glycogen levels in these tissues. The novel glycogen regulation by the sAC-cAMP-Epac1 signaling described here can be exploited to induce glycogen breakdown in tissues with pathologic glycogen accumulation to preserve organ functions. Finally, glycogen also plays an important role in tumorigenesis; the "clear cell" subtype of cancers of various tissues (e.g. clear cell renal cell carcinoma) are recognized for their glycogen-enriched cytoplasm histologically and aggressive behaviors clinically [97]. Cancer cells can utilize glycogen for proliferation, preventing premature senescence, and for metastasis [98,99]. Thus, the sAC-cAMP-Epac1 signaling could be further investigated for its potential as an anti-cancer strategy.

In summary, our data show that sAC-derived cAMP and tmAC-derived cAMP function within their respective, independent signaling microdomains and have opposite effects on glycogenolysis: the sAC-cAMP-Epac1 signaling suppresses glycogenolysis while the tmAC-cAMP-PKA signaling promotes glycogenolysis. While the hormone-regulated tmAC-cAMP-PKA mediates glycogenolysis in cells specialized in glycogen storage, we suggest that sAC-cAMP-Epac1 signaling regulates glycogenolysis independently of hormonal signaling to maintain energy homeostasis in both specialized and non-specialized cells. From the viewpoint of autonomous cellular metabolism, the cellular levels of ATP, bicarbonate (an index of Krebs cycle activity), and local $[Ca^{2+}]$ feed back to the sAC-cAMP-Epac1 signaling to prevent unnecessary glycogenolysis and wasteful lactate secretion during glucose starvation and, in some cell types, also in the presence of glucose. Our data strongly underscore the versatility of cAMP signaling and the concept of signaling microdomains, where adenylyl cyclases, cAMP-degrading phosphodiesterases, cAMP effectors, and downstream targets together maintain the spatial and functional specificity of different cAMP signaling within a cell [7,20].

5. Conclusions

Our study shows that, in a variety of cell types, cAMP generated by soluble adenylyl cyclase in the cytosol signals via the cAMP effector Epac1 to suppresses glycogen breakdown while cAMP generated by the transmembrane adenylyl cyclases located at the plasma membrane signals via the cAMP effector PKA to promote glycogen breakdown. Our data highlight the importance of cAMP microdomain organization for distinct metabolic regulation and establish sAC as a novel regulator of glycogen metabolism.

CRediT authorship contribution statement

Paulo F.V. Bizerra: Investigation, Formal analysis, Validation, Visualization, Writing – review & editing, Funding acquisition. **Eduardo H. Gilglioni:** Investigation, Formal analysis, Writing – review & editing. **Hang Lam Li:** Investigation, Formal analysis, Writing – review & editing. **Simei Go:** Investigation, Formal analysis, Writing – review & editing. **Ronald P.J. Oude Elferink:** Conceptualization, Writing – review & editing, Supervision, Funding acquisition. **Arthur J. Verhoeven:** Conceptualization, Investigation, Formal analysis, Writing – original draft, Supervision. **Jung-Chin Chang:** Conceptualization, Investigation, Formal analysis, Visualization, Writing – original draft, Supervision, Funding acquisition.

Declaration of competing interest

The authors declare the following financial interests/personal relationships which may be considered as potential competing interests: Ronald Oude Elferink reports financial support was provided by Dutch Cancer Society. Jung-Chin Chang reports financial support was provided by Amsterdam Gastroenterology Endocrinology Metabolism.

Data availability

Data will be made available on request.

Acknowledgments

Ronald Oude Elferink was supported by grant #11652-2018-1 from the Dutch Cancer Foundation (KWF/Alpe d'HuZes). Jung-Chin Chang was supported by AGEM Talent Development Grant of the Amsterdam Gastroenterology, Endocrinology & Metabolism Research Institute. Paulo F.V. Bizerra was supported by the Brazil National Council for Scientific and Technological Development (CNPq) fellowship. The authors thank Dr. D. de Korte (Sanquin Blood Foundation, Amsterdam, the Netherlands) for performing the analysis of adenylate nucleotides. The authors thank Suzanne Duijst (Tytgat Institute for Liver and Intestinal Research, Amsterdam UMC, the Netherlands) for assisting in the primary mouse hepatocyte isolation and Kam S. Ho-Mok (Tytgat Institute for Liver and Intestinal Research, Amsterdam UMC, the Netherlands) for assisting in immunoblotting.

Appendix A. Supplementary data

Supplementary data to this article can be found online at https://doi.org/10.1016/j.bbamcr.2023.119585.

References

[1] E.W. Sutherland, T.W. Rall, Fractionation and characterization of a cyclic adenine ribonucleotide formed by tissue particles, J. Biol. Chem. 232 (2) (1958) 1077–1091.
[2] E.W. Sutherland, T.W. Rall, The properties of an adenine ribonucleotide produced with cellular particles, ATP, Mg++, and epinephrine or glucagon, J. Am. Chem. Soc. 79 (13) (1957) 3608.
[3] J. Berthet, T.W. Rall, E.W. Sutherland, The relationship of epinephrine and glucagon to liver phosphorylase. IV. Effect of epinephrine and glucagon on the reactivation of phosphorylase in liver homogenates, J. Biol. Chem. 224 (1) (1957) 463–475.
[4] J. Hanoune, N. Defer, Regulation and role of adenylyl cyclase isoforms, Annu. Rev. Pharmacol. Toxicol. 41 (2001) 145–174.
[5] J. Buck, M.L. Sinclair, L. Schapal, M.J. Cann, L.R. Levin, Cytosolic adenylyl cyclase defines a unique signaling molecule in mammals, Proc. Natl. Acad. Sci. U. S. A. 96 (1) (1999) 79–84.
[6] Y. Chen, M.J. Cann, T.N. Litvin, V. Iourgenko, M.L. Sinclair, L.R. Levin, J. Buck, Soluble adenylyl cyclase as an evolutionarily conserved bicarbonate sensor, Science 289 (5479) (2000) 625–628.
[7] M. Kamenetsky, S. Middelhaufe, E.M. Bank, L.R. Levin, J. Buck, C. Steegborn, Molecular details of cAMP generation in mammalian cells: a tale of two systems, J. Mol. Biol. 362 (4) (2006) 623–639.
[8] T.N. Litvin, M. Kamenetsky, A. Zarifyan, J. Buck, L.R. Levin, Kinetic properties of "soluble" adenylyl cyclase. Synergism between calcium and bicarbonate, J. Biol. Chem. 278 (18) (2003) 15922–15926.
[9] W. Geng, Z. Wang, J. Zhang, B.Y. Reed, C.Y. Pak, O.W. Moe, Cloning and characterization of the human soluble adenylyl cyclase, Am. J. Phys. Cell Phys. 288 (6) (2005) C1305–C1316.
[10] S. Kleinboelting, A. Diaz, S. Moniot, J. van den Heuvel, M. Weyand, L.R. Levin, J. Buck, C. Steegborn, Crystal structures of human soluble adenylyl cyclase reveal mechanisms of catalysis and of its activation through bicarbonate, Proc. Natl. Acad. Sci. U. S. A. 111 (10) (2014) 3727–3732.
[11] J.H. Zippin, Y. Chen, S.G. Straub, K.C. Hess, A. Diaz, D. Lee, P. Tso, G.G. Holz, G. W. Sharp, L.R. Levin, J. Buck, CO2/HCO3(−)- and calcium-regulated soluble adenylyl cyclase as a physiological ATP sensor, J. Biol. Chem. 288 (46) (2013) 33283–33291.
[12] J.H. Zippin, Y. Chen, P. Nahirney, M. Kamenetsky, M.S. Wuttke, D.A. Fischman, L. R. Levin, J. Buck, Compartmentalization of bicarbonate-sensitive adenylyl cyclase in distinct signaling microdomains, FASEB J. 17 (1) (2003) 82–84.
[13] R. Acin-Perez, E. Salazar, M. Kamenetsky, J. Buck, L.R. Levin, G. Manfredi, Cyclic AMP produced inside mitochondria regulates oxidative phosphorylation, Cell Metab. 9 (3) (2009) 265–276.
[14] M. Kobayashi, J. Buck, L.R. Levin, Conservation of functional domain structure in bicarbonate-regulated "soluble" adenylyl cyclases in bacteria and eukaryotes, Dev. Genes Evol. 214 (10) (2004) 503–509.
[15] R. Fredriksson, H.B. Schioth, The repertoire of G-protein-coupled receptors in fully sequenced genomes, Mol. Pharmacol. 67 (5) (2005) 1414–1425.
[16] G. Di Benedetto, E. Scalzotto, M. Mongillo, T. Pozzan, Mitochondrial ca(2)(+) uptake induces cyclic AMP generation in the matrix and modulates organelle ATP levels, Cell Metab. 17 (6) (2013) 965–975.
[17] B.S. Jaiswal, M. Conti, Calcium regulation of the soluble adenylyl cyclase expressed in mammalian spermatozoa, Proc. Natl. Acad. Sci. U. S. A. 100 (19) (2003) 10676–10681.
[18] L.R. Levin, J. Buck, Physiological roles of acid-base sensors, Annu. Rev. Physiol. 77 (2015) 347–362.
[19] J.C. Chang, S. Go, E.H. Gilglioni, S. Duijst, D.M. Panneman, R.J. Rodenburg, H. L. Li, H.L. Huang, L.R. Levin, J. Buck, A.J. Verhoeven, R.P.J. Oude Elferink, Soluble adenylyl cyclase regulates the cytosolic NADH/NAD(+) redox state and the bioenergetic switch between glycolysis and oxidative phosphorylation, Biochim. Biophys. Acta Bioenerg. 2021 (4) (1862) 148367.
[20] K. Lefkimmiatis, M. Zaccolo, cAMP signaling in subcellular compartments, Pharmacol. Ther. 143 (3) (2014) 295–304.
[21] S.R. Agarwal, R.T. Sherpa, K.S. Moshal, R.D. Harvey, Compartmentalized cAMP signaling in cardiac ventricular myocytes, Cell. Signal. 89 (2022) 110172.
[22] S.E. Anton, C. Kayser, I. Maiellaro, K. Nemec, J. Moller, A. Koschinski, M. Zaccolo, P. Annibale, M. Falcke, M.J. Lohse, A. Bock, Receptor-associated independent cAMP nanodomains mediate spatiotemporal specificity of GPCR signaling, Cell 185 (7) (2022) 1130–1142 (e11).
[23] S.R. Agarwal, C.E. Clancy, R.D. Harvey, Mechanisms restricting diffusion of intracellular cAMP, Sci. Rep. 6 (2016) 19577.
[24] M. Zaccolo, T. Pozzan, Discrete microdomains with high concentration of cAMP in stimulated rat neonatal cardiac myocytes, Science 295 (5560) (2002) 1711–1715.
[25] J. Jurevicius, R. Fischmeister, cAMP compartmentation is responsible for a local activation of cardiac Ca2+ channels by beta-adrenergic agonists, Proc. Natl. Acad. Sci. U. S. A. 93 (1) (1996) 295–299.
[26] A. Bock, P. Annibale, C. Konrad, A. Hannawacker, S.E. Anton, I. Maiellaro, U. Zabel, S. Sivaramakrishnan, M. Falcke, M.J. Lohse, Optical mapping of cAMP signaling at the nanometer scale, Cell 182 (6) (2020) 1519–1530 (e17).
[27] J.Z. Zhang, T.W. Lu, L.M. Stolerman, B. Tenner, J.R. Yang, J.F. Zhang, M. Falcke, P. Rangamani, S.S. Taylor, S. Mehta, J. Zhang, Phase separation of a PKA regulatory subunit controls cAMP compartmentation and oncogenic signaling, Cell 182 (6) (2020) 1531–1544 (e15).
[28] G. Pidoux, K. Tasken, Specificity and spatial dynamics of protein kinase a signaling organized by A-kinase-anchoring proteins, J. Mol. Endocrinol. 44 (5) (2010) 271–284.
[29] M. Zaccolo, A. Zerio, M.J. Lobo, Subcellular organization of the cAMP signaling pathway, Pharmacol. Rev. 73 (1) (2021) 278–309.
[30] J.C. Chang, S. Go, D.R. de Waart, P. Munoz-Garrido, U. Beuers, C.C. Paulusma, R. Oude Elferink, Soluble adenylyl cyclase regulates bile salt-induced apoptosis in human cholangiocytes, Hepatology 64 (2) (2016) 522–534.
[31] S. Kumar, S. Kostin, J.P. Flacke, H.P. Reusch, Y. Ladilov, Soluble adenylyl cyclase controls mitochondria-dependent apoptosis in coronary endothelial cells, J. Biol. Chem. 284 (22) (2009) 14760–14768.
[32] B. Obiako, W. Calchary, N. Xu, R. Kunstadt, B. Richardson, J. Nix, S.L. Sayner, Bicarbonate disruption of the pulmonary endothelial barrier via activation of endogenous soluble adenylyl cyclase, isoform 10, Am. J. Phys. Lung Cell. Mol. Phys. 305 (2) (2013) L185–L192.
[33] S.L. Sayner, D.W. Frank, J. King, H. Chen, J. VandeWaa, T. Stevens, Paradoxical cAMP-induced lung endothelial hyperpermeability revealed by Pseudomonas aeruginosa ExoY, Circ. Res. 95 (2) (2004) 196–203.
[34] E.H. Fischer, E.G. Krebs, Conversion of phosphorylase b to phosphorylase a in muscle extracts, J. Biol. Chem. 216 (1) (1955) 121–132.
[35] D.A. Walsh, J.P. Perkins, E.G. Krebs, An adenosine 3′,5′-monophosphate-dependant protein kinase from rabbit skeletal muscle, J. Biol. Chem. 243 (13) (1968) 3763–3765.
[36] E. Jakobsen, J.V. Andersen, S.K. Christensen, O. Siamka, M.R. Larsen, H. S. Waagepetersen, B.I. Aldana, L.K. Bak, Pharmacological inhibition of mitochondrial soluble adenylyl cyclase in astrocytes causes activation of AMP-activated protein kinase and induces breakdown of glycogen, Glia 69 (12) (2021) 2828–2844.
[37] H.B. Choi, G.R. Gordon, N. Zhou, C. Tai, R.L. Rungta, J. Martinez, T.A. Milner, J. K. Ryu, J.G. McLarnon, M. Tresguerres, L.R. Levin, J. Buck, B.A. MacVicar, Metabolic communication between astrocytes and neurons via bicarbonate-responsive soluble adenylyl cyclase, Neuron 75 (6) (2012) 1094–1104.
[38] S.A. Grubman, R.D. Perrone, D.W. Lee, S.L. Murray, L.C. Rogers, L.I. Wolkoff, A. E. Mulberg, V. Cherington, D.M. Jefferson, Regulation of intracellular pH by immortalized human intrahepatic biliary epithelial cell lines, Am. J. Phys. 266 (6 Pt 1) (1994) G1060–G1070.
[39] S.A. Mookerjee, A.A. Gerencser, D.G. Nicholls, M.D. Brand, Quantifying intracellular rates of glycolytic and oxidative ATP production and consumption using extracellular flux measurements, J. Biol. Chem. 292 (17) (2017) 7189–7207.
[40] S.A. Mookerjee, R.L. Goncalves, A.A. Gerencser, D.G. Nicholls, M.D. Brand, The contributions of respiration and glycolysis to extracellular acid production, Biochim. Biophys. Acta 1847 (2) (2015) 171–181.
[41] E.H. Gilglioni, J.-C. Chang, S. Duijst, S. Go, A.A.A. Adam, R. Hoekstra, A. J. Verhoeven, E.L. Ishii-Iwamoto, R.P.J. Oude Elferink, Improved oxygenation dramatically alters metabolism and gene expression in cultured primary mouse hepatocytes, Hepatol. Commun. 2 (3) (2018) 299–312.
[42] I.J. Bontekoe, P.F. van der Meer, K. van den Hurk, A.J. Verhoeven, D. de Korte, Platelet storage performance is consistent by donor: a pilot study comparing "good" and "poor" storing platelets, Transfusion 57 (10) (2017) 2373–2380.
[43] D.E. Atkinson, G.M. Walton, Adenosine triphosphate conservation in metabolic regulation. Rat liver citrate cleavage enzyme, J. Biol. Chem. 242 (13) (1967) 3239–3241.
[44] J. Moffat, D.A. Grueneberg, X. Yang, S.Y. Kim, A.M. Kloepfer, G. Hinkle, B. Piqani, T.M. Eisenhaure, B. Luo, J.K. Grenier, A.E. Carpenter, S.Y. Foo, S.A. Stewart, B. R. Stockwell, N. Hacohen, W.C. Hahn, E.S. Lander, D.M. Sabatini, D.E. Root, A lentiviral RNAi library for human and mouse genes applied to an arrayed viral high-content screen, Cell 124 (6) (2006) 1283–1298.
[45] S. Go, H.L. Li, J.C. Chang, A.J. Verhoeven, R. Elferink, Cholangiocytes express an isoform of soluble adenylyl cyclase that is N-linked glycosylated and secreted in extracellular vesicles, Traffic 24 (9) (2023) 413–430.

[46] L. Ramos-Espiritu, S. Kleinboelting, F.A. Navarrete, A. Alvau, P.E. Visconti, F. Valsecchi, A. Starkov, G. Manfredi, H. Buck, C. Adura, J.H. Zippin, J. van den Heuvel, J.F. Glickman, C. Steegborn, L.R. Levin, J. Buck, Discovery of LRE1 as a specific and allosteric inhibitor of soluble adenylyl cyclase, Nat. Chem. Biol. 12 (10) (2016) 838–844.
[47] W.H. Martin, D.J. Hoover, S.J. Armento, I.A. Stock, R.K. McPherson, D.E. Danley, R.W. Stevenson, E.J. Barrett, J.L. Treadway, Discovery of a human liver glycogen phosphorylase inhibitor that lowers blood glucose in vivo, Proc. Natl. Acad. Sci. U. S. A. 95 (4) (1998) 1776–1781.
[48] M. Rousset, A. Zweibaum, J. Fogh, Presence of glycogen and growth-related variations in 58 cultured human tumor cell lines of various tissue origins, Cancer Res. 41 (3) (1981) 1165–1170.
[49] J.P. Flacke, H. Flacke, A. Appukuttan, R.J. Palisaar, J. Noldus, B.D. Robinson, H. P. Reusch, J.H. Zippin, Y. Ladilov, Type 10 soluble adenylyl cyclase is overexpressed in prostate carcinoma and controls proliferation of prostate cancer cells, J. Biol. Chem. 288 (5) (2013) 3126–3135.
[50] Y. Onodera, J.M. Nam, M.J. Bissell, Increased sugar uptake promotes oncogenesis via EPAC/RAP1 and O-GlcNAc pathways, J. Clin. Invest. 124 (1) (2014) 367–384.
[51] F. Valsecchi, C. Konrad, M. D'Aurelio, L.S. Ramos-Espiritu, A. Stepanova, S. R. Burstein, A. Galkin, J. Magrane, A. Starkov, J. Buck, L.R. Levin, G. Manfredi, Distinct intracellular sAC-cAMP domains regulate ER Ca(2+) signaling and OXPHOS function, J. Cell Sci. 130 (21) (2017) 3713–3727.
[52] D. Courilleau, M. Bisserier, J.C. Jullian, A. Lucas, P. Bouyssou, R. Fischmeister, J. P. Blondeau, F. Lezoualc'h, Identification of a tetrahydroquinoline analog as a pharmacological inhibitor of the cAMP-binding protein Epac, J. Biol. Chem. 287 (53) (2012) 44192–44202.
[53] T. Tsalkova, F.C. Mei, S. Li, O.G. Chepurny, C.A. Leech, T. Liu, G.G. Holz, V. L. Woods Jr., X. Cheng, Isoform-specific antagonists of exchange proteins directly activated by cAMP, Proc. Natl. Acad. Sci. U. S. A. 109 (45) (2012) 18613–18618.
[54] D. De Rasmo, A. Signorile, A. Santeramo, M. Larizza, P. Lattanzio, G. Capitanio, S. Papa, Intramitochondrial adenylyl cyclase controls the turnover of nuclear-encoded subunits and activity of mammalian complex I of the respiratory chain, Biochim. Biophys. Acta 1853 (1) (2015) 183–191.
[55] S. Heinz, A. Freyberger, B. Lawrenz, L. Schladt, G. Schmuck, H. Ellinger-Ziegelbauer, Mechanistic investigations of the mitochondrial complex I inhibitor rotenone in the context of pharmacological and safety evaluation, Sci. Rep. 7 (2017) 45465.
[56] D. Carling, D.G. Hardie, The substrate and sequence specificity of the AMP-activated protein kinase. Phosphorylation of glycogen synthase and phosphorylase kinase, Biochim. Biophys. Acta 1012 (1) (1989) 81–86.
[57] L. Bultot, B. Guigas, A. Von Wilamowitz-Moellendorff, L. Maisin, D. Vertommen, N. Hussain, M. Beullens, J.J. Guinovart, M. Foretz, B. Viollet, K. Sakamoto, L. Hue, M.H. Rider, AMP-activated protein kinase phosphorylates and inactivates liver glycogen synthase, Biochem. J. 443 (1) (2012) 193–203.
[58] L.N. Johnson, Glycogen phosphorylase: control by phosphorylation and allosteric effectors, FASEB J. 6 (6) (1992) 2274–2282.
[59] C. Nolan, W.B. Novoa, E.G. Krebs, E.H. Fischer, Further studies on the site phosphorylated in the phosphorylase B to a reaction, Biochemistry 3 (1964) 542–551.
[60] D.L. Beene, J.D. Scott, A-kinase anchoring proteins take shape, Curr. Opin. Cell Biol. 19 (2) (2007) 192–198.
[61] F.C. Mei, J. Qiao, O.M. Tsygankova, J.L. Meinkoth, L.A. Quilliam, X. Cheng, Differential signaling of cyclic AMP: opposing effects of exchange protein directly activated by cyclic AMP and cAMP-dependent protein kinase on protein kinase B activation, J. Biol. Chem. 277 (13) (2002) 11497–11504.
[62] S.R. Nelson, D.W. Schulz, J.V. Passonneau, O.H. Lowry, Control of glycogen levels in brain, J. Neurochem. 15 (11) (1968) 1271–1279.
[63] J. Duran, A. Gruart, M. Garcia-Rocha, J.M. Delgado-Garcia, J.J. Guinovart, Glycogen accumulation underlies neurodegeneration and autophagy impairment in Lafora disease, Hum. Mol. Genet. 23 (12) (2014) 3147–3156.
[64] M. Nannipieri, A. Lanfranchi, D. Santerini, C. Catalano, G. Van de Werve, E. Ferrannini, Influence of long-term diabetes on renal glycogen metabolism in the rat, Nephron 87 (1) (2001) 50–57.
[65] C.A. Schneider, V.T. Nguyen, H. Taegtmeyer, Feeding and fasting determine postischemic glucose utilization in isolated working rat hearts, Am. J. Phys. 260 (2 Pt 2) (1991) H542–H548.
[66] E. Wertheimer, Glycogen in adipose tissue, J. Physiol. 103 (4) (1945) 359–366.
[67] A.E. Renold, A. Marble, D.W. Fawcett, Action of insulin on deposition of glycogen and storage of fat in adipose tissue, Endocrinology 46 (1) (1950) 55–66.
[68] J. Ma, K. Wei, J. Liu, K. Tang, H. Zhang, L. Zhu, J. Chen, F. Li, P. Xu, J. Chen, J. Liu, H. Fang, L. Tang, D. Wang, L. Zeng, W. Sun, J. Xie, Y. Liu, B. Huang, Glycogen metabolism regulates macrophage-mediated acute inflammatory responses, Nat. Commun. 11 (1) (2020) 1769.
[69] M.E. Gibbs, D.G. Anderson, L. Hertz, Inhibition of glycogenolysis in astrocytes interrupts memory consolidation in young chickens, Glia 54 (3) (2006) 214–222.
[70] A. Suzuki, S.A. Stern, O. Bozdagi, G.W. Huntley, R.H. Walker, P.J. Magistretti, C. M. Alberini, Astrocyte-neuron lactate transport is required for long-term memory formation, Cell 144 (5) (2011) 810–823.
[71] M. Karlsson, C. Zhang, L. Mear, W. Zhong, A. Digre, B. Katona, E. Sjostedt, L. Butler, J. Odeberg, P. Dusart, F. Edfors, P. Oksvold, K. von Feilitzen, M. Zwahlen, M. Arif, O. Altay, X. Li, M. Ozcan, A. Mardinoglu, L. Fagerberg, J. Mulder, Y. Luo, F. Ponten, M. Uhlen, C. Lindskog, A single-cell type transcriptomics map of human tissues, Sci. Adv. 7 (31) (2021).
[72] R.J. Brushia, D.A. Walsh, Phosphorylase kinase: the complexity of its regulation is reflected in the complexity of its structure, Front. Biosci. 4 (1999) D618–D641.
[73] L. Fazal, M. Laudette, S. Paula-Gomes, S. Pons, C. Conte, F. Tortosa, P. Sicard, Y. Sainte-Marie, M. Bisserier, O. Lairez, A. Lucas, J. Roy, B. Ghaleb, J. Fauconnier, J. Mialet-Perez, F. Lezoualc'h, Multifunctional mitochondrial Epac1 controls myocardial cell death, Circ. Res. 120 (4) (2017) 645–657.
[74] M. Laudette, Y. Sainte-Marie, G. Cousin, D. Bergonnier, I. Belhabib, S. Brun, K. Formoso, L. Laib, F. Tortosa, C. Bergoglio, B. Marcheix, J. Boren, O. Lairez, J. Fauconnier, A. Lucas, J. Mialet-Perez, C. Moro, F. Lezoualc'h, Cyclic AMP-binding protein Epac1 acts as a metabolic sensor to promote cardiomyocyte lipotoxicity, Cell Death Dis. 12 (9) (2021) 824.
[75] S. Mangmool, A.K. Shukla, H.A. Rockman, Beta-Arrestin-dependent activation of Ca(2+)/calmodulin kinase II after beta(1)-adrenergic receptor stimulation, J. Cell Biol. 189 (3) (2010) 573–587.
[76] M. Fivaz, T. Meyer, Reversible intracellular translocation of KRas but not HRas in hippocampal neurons regulated by Ca2+/calmodulin, J. Cell Biol. 170 (3) (2005) 429–441.
[77] D.S. Carter, S.N. Haider, R.E. Blair, L.S. Deshpande, S. Sombati, R.J. DeLorenzo, Altered calcium/calmodulin kinase II activity changes calcium homeostasis that underlies epileptiform activity in hippocampal neurons in culture, J. Pharmacol. Exp. Ther. 319 (3) (2006) 1021–1031.
[78] N.M. Ashpole, W. Song, T. Brustovetsky, E.A. Engleman, N. Brustovetsky, T. R. Cummins, A. Hudmon, Calcium/calmodulin-dependent protein kinase II (CaMKII) inhibition induces neurotoxicity via dysregulation of glutamate/calcium signaling and hyperexcitability, J. Biol. Chem. 287 (11) (2012) 8495–8506.
[79] P. Singh, M. Salih, J.J. Leddy, B.S. Tuana, The muscle-specific calmodulin-dependent protein kinase assembles with the glycolytic enzyme complex at the sarcoplasmic reticulum and modulates the activity of glyceraldehyde-3-phosphate dehydrogenase in a Ca2+/calmodulin-dependent manner, J. Biol. Chem. 279 (34) (2004) 35176–35182.
[80] X. Zhang, X. Wang, Z. Yuan, S.J. Radford, C. Liu, S.K. Libutti, X.F.S. Zheng, Amino acids-Rab1A-mTORC1 signaling controls whole-body glucose homeostasis, Cell Rep. 34 (11) (2021) 108830.
[81] J.D. Thomas, Y.J. Zhang, Y.H. Wei, J.H. Cho, L.E. Morris, H.Y. Wang, X.F. Zheng, Rab1A is an mTORC1 activator and a colorectal oncogene, Cancer Cell 26 (5) (2014) 754–769.
[82] R. Pal, Y. Xiong, M. Sardiello, Abnormal glycogen storage in tuberous sclerosis complex caused by impairment of mTORC1-dependent and -independent signaling pathways, Proc. Natl. Acad. Sci. U. S. A. 116 (8) (2019) 2977–2986.
[83] L. Meikle, J.R. McMullen, M.C. Sherwood, A.S. Lader, V. Walker, J.A. Chan, D. J. Kwiatkowski, A mouse model of cardiac rhabdomyoma generated by loss of Tsc1 in ventricular myocytes, Hum. Mol. Genet. 14 (3) (2005) 429–435.
[84] K.F. Chan, D.J. Graves, Isolation and physicochemical properties of active complexes of rabbit muscle phosphorylase kinase, J. Biol. Chem. 257 (10) (1982) 5939–5947.
[85] P. Newsholme, K.L. Angelos, D.A. Walsh, High and intermediate affinity calmodulin binding domains of the alpha and beta subunits of phosphorylase kinase and their potential role in phosphorylation-dependent activation of the holoenzyme, J. Biol. Chem. 267 (2) (1992) 810–818.
[86] A. Cheng, T.J. Fitzgerald, G.M. Carlson, Adenosine 5′-diphosphate as an allosteric effector of phosphorylase kinase from rabbit skeletal muscle, J. Biol. Chem. 260 (4) (1985) 2535–2542.
[87] T.R. Soderling, A.K. Srivastava, M.A. Bass, B.S. Khatra, Phosphorylation and inactivation of glycogen synthase by phosphorylase kinase, Proc. Natl. Acad. Sci. U. S. A. 76 (6) (1979) 2536–2540.
[88] N. Wu, B. Zheng, A. Shaywitz, Y. Dagon, C. Tower, G. Bellinger, C.H. Shen, J. Wen, J. Asara, T.E. McGraw, B.B. Kahn, L.C. Cantley, AMPK-dependent degradation of TXNIP upon energy stress leads to enhanced glucose uptake via GLUT1, Mol. Cell 49 (6) (2013) 1167–1175.
[89] K. Barnes, J.C. Ingram, O.H. Porras, L.F. Barros, E.R. Hudson, L.G. Fryer, F. Foufelle, D. Carling, D.G. Hardie, S.A. Baldwin, Activation of GLUT1 by metabolic and osmotic stress: potential involvement of AMP-activated protein kinase (AMPK), J. Cell Sci. 115 (Pt 11) (2002) 2433–2442.
[90] R.W. Hunter, J.T. Treebak, J.F. Wojtaszewski, K. Sakamoto, Molecular mechanism by which AMP-activated protein kinase activation promotes glycogen accumulation in muscle, Diabetes 60 (3) (2011) 766–774.
[91] M. Arad, D.W. Benson, A.R. Perez-Atayde, W.J. McKenna, E.A. Sparks, R.J. Kanter, K. McGarry, J.G. Seidman, C.E. Seidman, Constitutively active AMP kinase mutations cause glycogen storage disease mimicking hypertrophic cardiomyopathy, J. Clin. Invest. 109 (3) (2002) 357–362.
[92] W.G. Aschenbach, M.F. Hirshman, N. Fujii, K. Sakamoto, K.F. Howlett, L. J. Goodyear, Effect of AICAR treatment on glycogen metabolism in skeletal muscle, Diabetes 51 (3) (2002) 567–573.
[93] M. Arad, I.P. Moskowitz, V.V. Patel, F. Ahmad, A.R. Perez-Atayde, D.B. Sawyer, M. Walter, G.H. Li, P.G. Burgon, C.T. Maguire, D. Stapleton, J.P. Schmitt, X.X. Guo, A. Pizard, S. Kupershmidt, D.M. Roden, C.I. Berul, C.E. Seidman, J.G. Seidman, Transgenic mice overexpressing mutant PRKAG2 define the cause of Wolff-Parkinson-White syndrome in glycogen storage cardiomyopathy, Circulation 107 (22) (2003) 2850–2856.
[94] H. Ozen, Glycogen storage diseases: new perspectives, World J. Gastroenterol. 13 (18) (2007) 2541–2553.
[95] J. Hicks, E. Wartchow, G. Mierau, Glycogen storage diseases: a brief review and update on clinical features, genetic abnormalities, pathologic features, and treatment, Ultrastruct. Pathol. 35 (5) (2011) 183–196.
[96] F. Nitschke, S.J. Ahonen, S. Nitschke, S. Mitra, B.A. Minassian, Lafora disease - from pathogenesis to treatment strategies, Nat. Rev. Neurol. 14 (10) (2018) 606–617.

[97] T. Khan, M.A. Sullivan, J.H. Gunter, T. Kryza, N. Lyons, Y. He, J.D. Hooper, Revisiting glycogen in cancer: a conspicuous and targetable enabler of malignant transformation, Front. Oncol. 10 (2020) 592455.
[98] M. Curtis, H.A. Kenny, B. Ashcroft, A. Mukherjee, A. Johnson, Y. Zhang, Y. Helou, R. Batlle, X. Liu, N. Gutierrez, X. Gao, S.D. Yamada, R. Lastra, A. Montag, N. Ahsan, J.W. Locasale, A.R. Salomon, A.R. Nebreda, E. Lengyel, Fibroblasts mobilize tumor cell glycogen to promote proliferation and metastasis, Cell Metab. 29 (1) (2019) 141–155 (e9).
[99] E. Favaro, K. Bensaad, M.G. Chong, D.A. Tennant, D.J. Ferguson, C. Snell, G. Steers, H. Turley, J.L. Li, U.L. Gunther, F.M. Buffa, A. McIntyre, A.L. Harris, Glucose utilization via glycogen phosphorylase sustains proliferation and prevents premature senescence in cancer cells, Cell Metab. 16 (6) (2012) 751–764.